2017

Academic Blade Geometries for Baseline Comparisons of Forced Vibration Response Predictions

James Little
University of Central Florida

ACADEMIC BLADE GEOMETRIES FOR BASELINE COMPARISONS OF FORCED VIBRATION RESPONSE PREDICTIONS

by

JAMES H. LITTLE II
B.S. University of Central Florida, 2015

A thesis submitted in partial fulfillment of the requirements
for the degree of Master of Science
in the Department of Mechanical and Aerospace Engineering
in the College of Engineering and Computer Science
at the University of Central Florida
Orlando, Florida

Spring Term
2017

Major Professor: Jeffrey L. Kauffman

ABSTRACT

Predicting the damping associated with underplatform dampers remains a challenge in turbomachinery blade and friction damper design. Turbomachinery blade forced response analysis methods usually rely on nonlinear codes and reduced order models to predict vibration characteristics of blades. Two academic blade geometries coupled with underplatform dampers are presented here for comparison of these model reduction and forced response simulation techniques. The two blades are representative of free-standing turbine blades and exhibit qualitatively similar behavior as highly-complex industrial blades. This thesis fully describes the proposed academic blade geometries and models; it further analyzes and predicts the blades forced response characteristics using the same procedure as industry blades. This analysis classifies the results in terms of resonance frequency, vibration amplitude, and damping over a range of aerodynamic excitation to examine the vibration behavior of the blade/damper system. Additionally, the analysis investigates the effect variations of the contact parameters (friction coefficient, damper / platform roughness and damper mass) have on the predicted blade vibration characteristics, with sensitivities to each parameter. Finally, an investigation of the number of modes retained in the reduced order model shows convergence behavior as well as providing additional data for comparison with alternative model reduction and forced response prediction methods. The academic blade models are shown to behave qualitatively similar to high fidelity industry blade models when the number of retained

modes in a modal analysis are varied and behave qualitatively similar under sensitives to design parameters.

I would like to dedicate this thesis to my family and friends for their love and support throughout and leading up to this experience. To my adviser Dr. Jeffrey L. Kauffman for his guidance and insightful feedback throughout this research and navigation of my academic career. I would also like to thank my lab-mates for their comradery during this experience.

ACKNOWLEDGMENTS

The author would like to acknowledge Dr. Stefan Schmitt, Mr. Matthias Huels and Mr. Ryan Villanueva for their support and feedback. The author would also like to acknowledge Siemens for providing funding for this research and permission to publish.

TABLE OF CONTENTS

LIST OF FIGURES

LIST OF TABLES

CHAPTER 1
INTRODUCTION

Figure 1.1: Example of Blade Failure. From ATSB

Turbomachinery blades experience large aerodynamic forces that if left unchecked, can lead to high vibration, reduced blade life and high-cycle fatigue; figure 1.1 shows one such example where the failure was attributed to high cycle fatigue. Turbomachinery manufacturers therefore need to ensure these vibrations remain below a safety limit for safe, reliable and cost effective power generation. A common method to reduce these vibrations is to couple turbine blades with underplatform dampers, which are friction dampers positioned beneath the the blade platforms between adjacent blades. These dampers reduce the vibrations caused by the dynamic loads expe-

rienced during operation by dissipating energy through friction at contact surfaces. As the blades vibrate, the underplatform damper slides under friction between two adjacent blades, thus dissipating energy from the blades. Although this idea seems simple, the behavior of these systems is rather complex and highly nonlinear. This complexity leads to a large computational cost when applied to the high-fidelity models commonly seen in industry where typical blade models contain thousands to even millions degrees of freedom. To reduce the size of the problem, reduced order models and nonlinear codes are used to attain the blade vibration characteristics while maintaining fidelity in the contact points to simulate blade vibration behavior. There are a multitude of methods which address model reduction and contact dynamics; however, it remains difficult to compare the performance of the methods across different blades which the results are presented from. The predicted forced vibration response of industry blade models are known to be affected by the number of retained modes in their reduced order models; figure 2.7 demonstrates this. This remains a critical factor in the analysis of high-fidelity blade models and is a key behavior the academic blade models presented here should mimic. The idea of the simpler academic blade models requiring a large number of modes retained in the modal analysis for convergence is intended to provide a medium for more a more fundamental investigation into the numerical stiffness being introduced during the model reduction process.

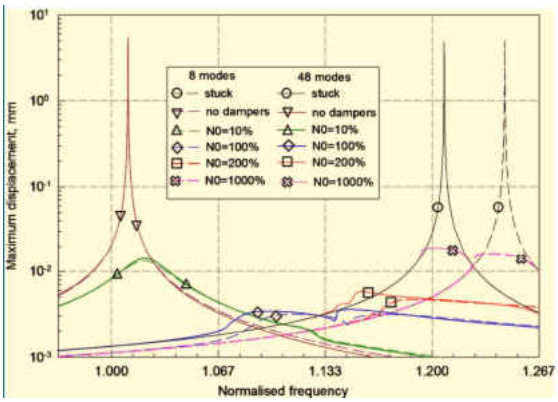

Figure 1.2: Example of Mode Dependent Forced Response. From [1]

Two academic turbine geometries coupled with underplatform dampers are presented which qualitatively exhibit similar vibration behavior as industry blade geometries and dampers. With the continued evolution of model reduction and contact dynamics modeling, these academic blades and dampers can assist in bridging the gap between academic and industry analyses. The two academic blades were constructed to cover a range of typical free-standing turbine blade designs used in gas turbines for power generation. One blade includes a broach angle, while the other does not and the blades span different length scales as well. The academic blades also utilize different platform angles. Additionally, each academic blade is accompanied with an asymmetric underplatform damper which are a widely used damper design in industry. The academic blade models above the platform area are simplistic in design due to only being interested in the modal properties of the profile. On the other hand, the blade root and platform region require a more rigorous physical definition given its importance in friction damping with the incorporation of underplatform dampers, where the damper makes contact with the blade.

The academic blade geometries presented here would act as a standard test case for academic studies, instead of relying on a new blade model or an industry blade. This paper describes the procedure to create the blades with a complete physical description and associated reduced order models. The blade models presented here were designed to be relatively simple compared to blades seen in industry so that they may be constructed using software readily available to academia, while still behaving qualitatively similar to the industry blades. The academic blade geometries presented here are analyzed using the same procedure as their industrial counterparts and the results are compared to validate the designs. The analysis procedure involves using a finite element package (ANSYS Mechanical APDL) to conduct a mode-based harmonic analysis of finite element models of the blades. The results of the modal analysis are then imported into a nonlinear damping code used in industry to examine the dynamic characteristics of the blade system. The forced vibration response results are presented in terms of sensitivities to variations in the contact interface parameters (such as the damper mass, contact surface roughness and the friction coefficient). The results are presented to act as a basis of comparison for future methods of forced response and damping studies.

Each academic blade has several corresponding reduced order models which are examined using the previously mentioned procedure in order to investigate the effect on the vibration behavior with respect to variations in the contact parameters . The reduced order models of the academic blade models are comprised of varying the number of retained modes in the modal analysis. The academic blade models will be considered successful if the blades require a large number of modes for convergence due to the poor coupling between the blade and underplatform regions since the

blade sections are simple cantilever beams. The goal is to demonstrate that the proposed academic blade models would be useful for further academic analysis techniques as a standard point of comparison in the forced response prediction of turbine blades.

This thesis is organized as follows. The next chapter provides some background in the field of friction damping research and contact modeling methods. The following chapter discusses the blade geometries with an overview on selection of design parameters, with sub sections on the design of each specific blade. Finally, the results of the forced responses are calculated using a nonlinear damping approach based on a code commonly used in industry, with the results to be used as a standard test case and a comparison of contact modeling in both industry and academia.

CHAPTER 2
BACKGROUND

2.1 Friction Damping

Friction dampers have been widely used in the turbomachinery community to reduce blade vibration for years. Underplatform dampers are one common friction damper which are placed underneath the blade platforms in between adjacent blades; figure 2.1 shows an example of the blade-damper system. As the blades vibrate, the relative motion between the damper and blade results in friction and the damper dissipates the energy of the blade.

A review article by Griffin provides a good overview of the advances in theoretical development of friction damping modeling and design of friction dampers, as well as recommendations for future work [9]. Griffin discusses recent advances in the numerical methods of analyzing frictionally damped systems such as the harmonic balance method. The harmonic balance method assumes excitaion and displacement of the system are harmonic and transforms the nonlinear problem into a set of nonlinear algebraic equations. This method is shown to need much less computational time then time inegration techniques and a promising method to caculate the forced vibration response of blades. Griffin then discusses developments in the modeling of friction, the most popular ones being a form of Coulomb friction model and the developments on microslip models. Microslip

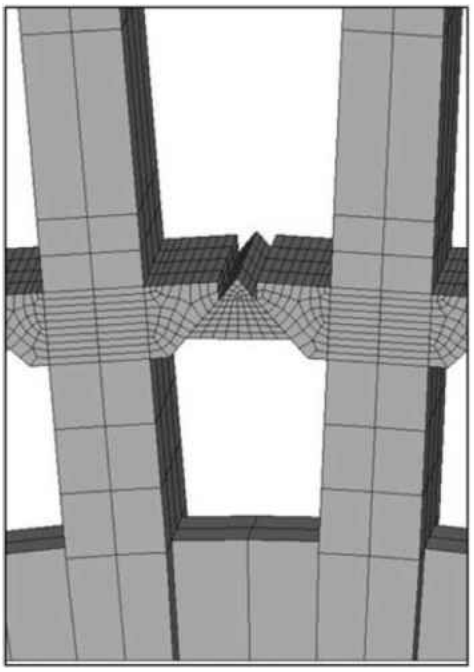

Figure 2.1: Turbine Blades with Underplatform Damper. From [2]

refers to the idea that friction occurs over a finite area of the contact and not the entire area as a whole, part of the area may be slipping while the rest is sticking. Models incorporating microslip indicate that dampers are effective over a wider range then those indicated with other methods. The work in damper optimization is discussed and the attempts at creating models to capture the contact dynamics between the underplatform dampers and blades. Work in the optimization of dampers demonstrates that when the damper is designed using a tuned blade assumption, this damper should work well for the mistuned systems which are common in application. Griffin concludes with recommending that future work be done to improve the modeling of single blade response, where the behavior between tuned and miss-tuned systems has been shown to correlate well. This would allow better damper designs and help eliminate need for laboratory tests.

Slater et al. conducted a review investigating recent advances in the forced response of bladed disk assemblies [10]. The authors discuss tuned analyses, mistuned analyses, damping and provide conclusions with recommendations for future work. The authors point out a need for a better understanding of the sensitivities of bladed disks to mode localization, instead of attempting to incorporate mistunning into the model.

Menq et al. focused on the modeling of friction between the damper and blade and eventually developed a model incorporating microslip to help identify the contact status of dampers [11]. The incorporation of microslip into friction models allowed better insight into the friction behavior experienced at contact interfaces and helps explain phenomena previously poorly understood. Menq et al. explore this by comparing the developed model to experiments in turbine blade damping [12]. The authors also develop a general method to calculate the steady-state response of friction contacts in which the contact pressure can vary dynamically with the motion of the system [11].

Greenwood and Williamson describe a theory of elastic contact that accounts for surface roughness and distinguishes between surfaces touching elastically and plastically [13]. The theory introduces a parameter called the plasticity index which is used as a criterion to identify when surfaces contact elastically or plastically. The authors experimentally measure the topography of many surfaces and find that the distribution of peaks can be accurately estimated with a Gaussian distribution. This leads to an idea that the friction between two surfaces is due to their surface topography and not material properties and thus pointing out the need to incorporate surface roughness of contacting interfaces.

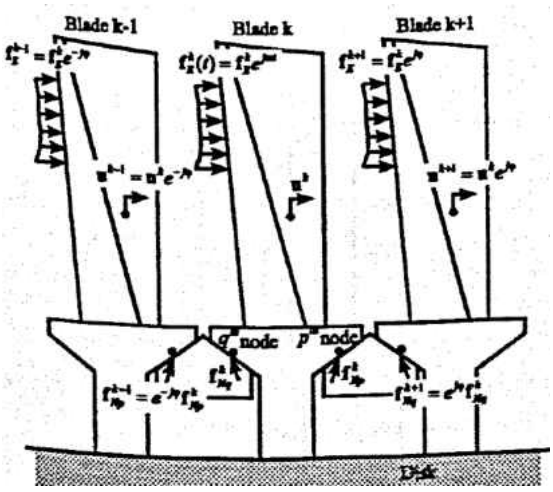

Figure 2.2: Turbine Blade with Wedge Damper Model. From [3]

In a series of paper Yang and Menq apply a friction model with microslip in the design of wedge dampers to calculate the forced response of a bladed disk to optimize the design and later compared with experimental results [14, 3]. The first paper discusses the the contact kinematics of a wedge damper; figure 2.2 shows a drawing of the blade and damper system used. The friction model utilizes force balance equations at the two coupled contact interfaces to analyze the state of contact (stick-slip); the criteria predicting this are derived analytically . The resulting friction and normal loads of the contact interfaces can then be predicted using the relative motion between the blades; this model was shown to be more accurate in predicting the damping and stiffness over a single interface model. This demonstrated the importance of using a multi-interface model to handle the coupling between the contact interfaces on underplatform dampers in the friction model. This model is then applied to a constrained turbine blade rig used by GE Aircraft Engines. The results demonstrated the ability of the proposed model to predict the vibration response when compared with experimental data.

Tworzydlo et al. discuss a new class of asperity-based models of contact interfaces which are a combination of finite element analysis of surface asperities and statistical techniques to predict the behavior of contact interfaces [15]. These new models are able to to produce realistic engineering contact interface surfaces and have been verified with experiments to predict the normal response of the interfaces well. The results confirmed previous observations that the contact area is proportional to the normal load, which was tested over a range of loads and surface roughness values. The models utilize numerical methods such as adaptive meshing and adaptive time-stepping to ensure high solution accuracy. These asperity-based models are an alternative to matching models to experimental results where measuring the surface compliance can be very difficult and the models only require material and roughness data.

Sextro describes a contact model which incorporates surface roughness and dry friciton in the calculation of the forced vibration response of a bladed disk with shrouds [16]. The surface roughness values of the two contacting surfaces are used to calculate an effective contact surface roughness in the contact model. The contact model is a two point contact model which incorporates the effective surface roughness in the prediction of the force-displacement behavior of contact. The predictions are compared with experimental data to verify the contact model and the model was applied to a bladed disk assembly. The results here demonstrate the importance of incorporating the effects of the contact surfaces roughness in the prediction of the behavior and resulting force-displacement relations.

Allara discusses a friction contact model to characterize non-sphereical interfaces following the Coulomb friction law, assuming a constant friction coefficient as well as normal load [17]. The

model computes the hysteresis loops of the contact tangential force against the relative displacement. The method presented is aimed at providing an estimate the effect the geometry of contact, loads, and material properties have on the contact behavior. However this method is only applicable when the contact area is of rectangular shape with the length much longer then the width.

Firrone and Zucca present a refined contact model which couples the static and dynamic equilibrium equations [4]. The coupling allows the maximum vibration amplitude of the system along with the stiffening of the structure to be predicted. This contact model is implemented with the Harmonic Balance Method and used to optimize friction dampers for bladed disks. This method is then applied to two configurations of turbine blades with friction contacts, one with blade root joints and the other with underplatform dampers to optimize the dampers; figure 2.3 shows the turbine blade model with underplatform dampers. The results are compared with classical contact models also discussed by the authors which do not couple the static and dynamic equilibrium equations. The comparisons revealed that the modeling of the coupling between the static and dynamic equilibrium equations is important in predicting the maximum vibration of the system and stiffening caused by the contact interfaces. The turbine blade models used by Firrone and Zucca are rather simplistic in design and similar to the blade models described later in this thesis [4]. The profiles of the blades above the platform are essentially cantilever beams and the platform regions follow the same profile as the models described in this thesis.

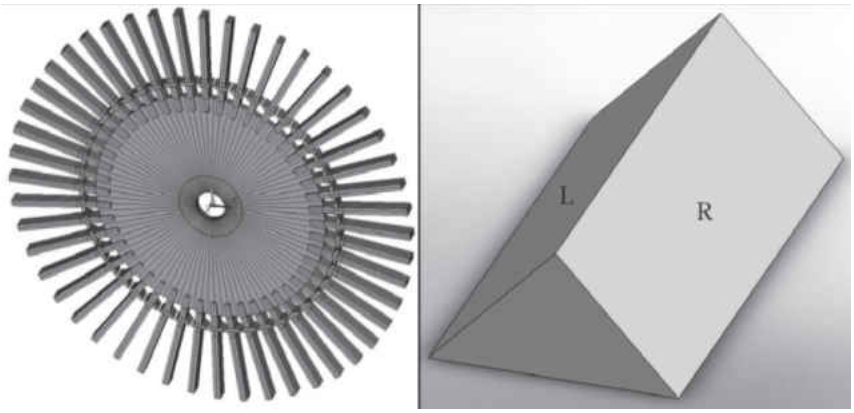

Figure 2.3: Bladed Disk and Wedge Damper. From [4]

2.2 Numerical Methods

There has been a large push recently in developing numerical methods to handle the simulation and computation of the contact dynamics associated with friction interfaces in turbomachinery. The multi-harmonic balance method is the most widely used to solve the nonlinear equations associated with the forced response of turbomachinery. The analysis of bladed disks with contact interfaces are usually carried out in the frequency domain for computational efficiency. This is achieved by representing the displacements as a sum of harmonic terms and transforms the nonlinear set of equations using the multi-harmonic balance method. Cardona et al. discuss the general procedure to solve nonlinear problems using the multi-harmonic balance method [18].

An alternative to using the Harmonic Balance Method is through the use of a dynamic lagrangian method adapted to be used in the frequency domain. Augmented Lagrangians are popular in the time domain formulation of contact problems. Nacivet et al. describe a dynamic Lagrangian

frequency-time method (DLFT) which is an adapted version of the augmented Lagrangians method for the frequency domain [5]. However the Lagrangians in this method are dynamic and based on the nonlinear contact forces from the equations of motion. The method is compared in three numerical examples to time integration preformed with the finite element software ABAQUS. The results demonstrated that the DLFT provides fast and accurate calculation of forced response with the most complex example being a system of beams each with a one dimensional friction damper; figure 2.4 shows the model. This method allows for the suppression of springs in the definition of contact elements which allows the method to be readily used with finite element software without the need for a special contact interface model. Although this model is well demonstrated on simple numerical examples, this method still needs to be verified with a more complex turbine blade model closer to those seen in industry.

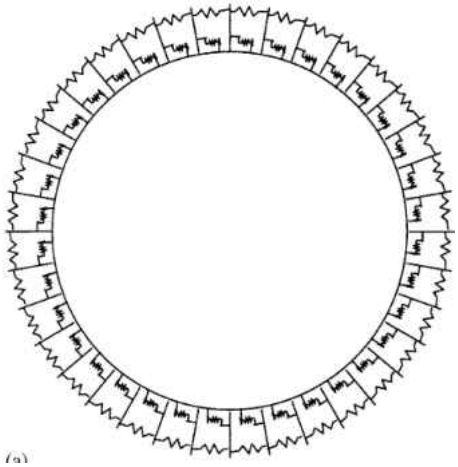

Figure 2.4: Bladed Disk and Damper Model. From [5]

Recently, researchers have been looking into nonlinear modal analysis which provide an alternative to model reduction methods needing to linearize systems [6, 1, 19]. Laxalde et al. presents

a method of modal analysis to analyze nonlinear systems and demonstrates it on a turbomachinery blade model [6]. The method described here is based on complex nonlinear modes and the formulation of the eigenvalue problem in the frequency domain to handle the contact. This method is then applied to an industrial compressor blade with dry friction at the blade root shown in figure 2.5. This method allows the nonlinear damping to be viewed immediately in addition to the excitation not being required to be known ahead of time. The use of nonlinear modal analysis allows the representation of systems with dissipative nonlinearities which are unable to be modeled effectively otherwise.

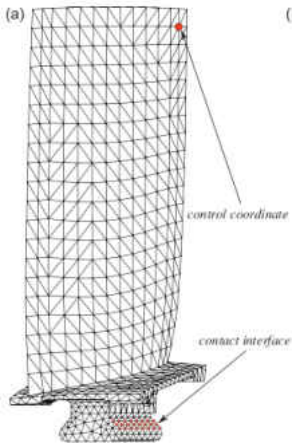

Figure 2.5: Industrial Compressor Blade Model. From [6]

In a series of papers Panning et al. describe a 3D point contact model which descretizes the contact area into point contacts and investigates underplatform damper design [20, 21, 22]. The first paper compares two different damper geometries, while the next paper investigates geometries and properties of the damper and blade platform. Then in the third paper, the authors demonstrate the need to treat different damper geometries with different theory, this is verified with experiments

and the nonlinear damping code DATAR which predicts the forced response of bladed disks with dampers and aids in friction damper design.

Within industry there have been numerous nonlinear damping codes developed to calculate the forced response of turbine blades. DATAR is one such example which was developed to aid in underplatform damper and is capable of handling a range of damper types [22]. DATAR utilizes contact stiffness terms to enforce contact which are related to the normal and tangential relative motions between the blade platform and underplatform damper. Siewert et al. describe the contact stiffness terms in more depth along with their calculation method [23]. DATAR couples physical parameters associated with the contact between the damper and blade along (such as damper mass, surface roughness, friction coefficient) with a modal representation of a tuned bladed disk model reduced order model. DATAR calculates the frequency response function of a tuned bladed disk with friction contacts (shrouds, underplatform dampers)

More recent research has demonstrated the potential for an augmented Lagrangian approach for enforcing contact to be more accurate at the same computational cost [7, 24, 25]. Herzog et al. compare two contact models; one using stiffness with a Coulomb friction law, the other with a Lagrangian formulation to enforce contact [7]. The contact models are applied to model a bladed disk with shroud contacts where the predicted damping, convergence and sensitives to inputs are compared; figure 2.6 shows the finite element model investigated. The blade model used in this study is rather simple in design compared to those seen in industry and to even the models presented in this thesis. The platform region of the blade is very simplistic, resembling a plate while the blade profile does have twist along its length to the shroud. However even the shroud is

very simplistic in design and 20 modes are retained in the modal analysis to achieve convergence of the forced response results.The authors reported that the two contact models produced similar results in the displacement and frequency for the forced response of a bladed disk. Additionally the Lagrangian formulation was much less sensitive to input parameters then using contact stiffness, which have a large impact and require careful selection.

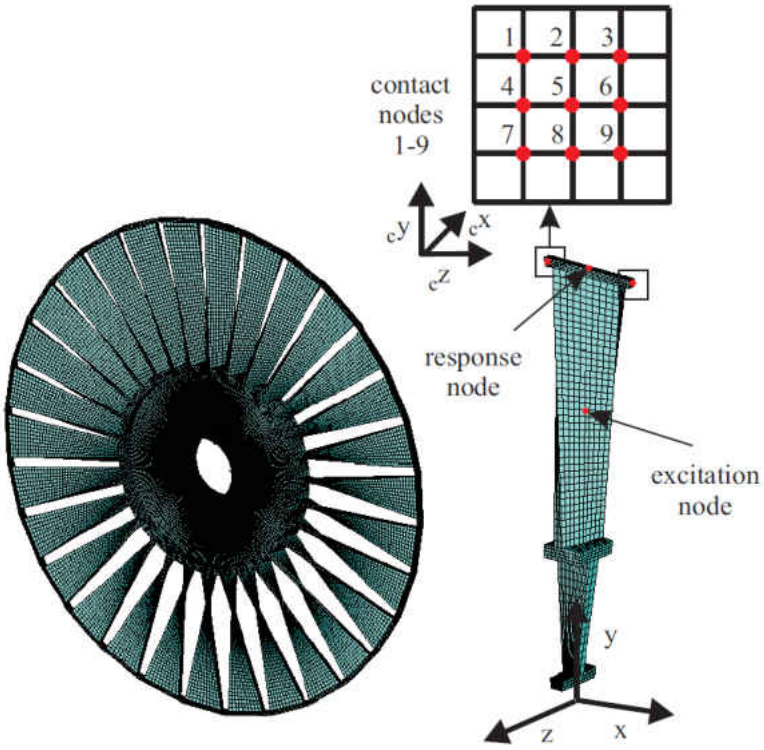

Figure 2.6: Shrouded Turbine Blade Finite Element Model. From [7]

Krack et al. describe a criterion to find the optimal design that is robust in regards to the uncertainty of system parameters of a shrouded bladed disk; the same model shown earlier in figure 2.6 [24]. The contact is modeled using a point contact model with a Dynamic Lagrangian method for enforcing contact. The criterion used to find the optimal design with uncertainty in-

volved employing statistical decision theory and the expected value of the probability of success, with respect to not exceeding a certain reference amplitude. It was found that the optimum contact interface load shifted about 25% compared to the designs without uncertainty modeling even when minor uncertainties are considered.

Krack et al. present a frequency domain method to compute periodic solutions of nonlinear ordinary differential equations [25]. The method is primarily for the analysis of systems with distinct states such as systems with contact interfaces where the contact state evolves over time. Additionally the derivatives of the solution up to the second order are able to derived analytically which is helpful for design. The method described is applied to two numerical examples of systems with dissipative nonlinearities and is shown to be superior in terms of accuracy and computation time to the commonly used Alternating-Frequency-Time scheme. However this method was only applied to very simple two degree of freedom and cantilever beam with friction contact at the free-end. While this method seems to have promise, it has yet to be implemented into a more complex systems such as turbomachinery.

2.3 Model Reduction

Contact interfaces in which friction occurs are highly nonlinear in behavior and require a certain amount of fidelity to capture their behavior. Turbomachinery systems usually contain numerous contact interfaces where friction occurs to dissipate unwanted vibrations during operation. In order to make the problem more computationally tractable, many researchers have focused on model

reduction techniques to bring the number of degrees of freedom in the system down to a more manageable level while maintaining as high accuracy as possible.

Petrov and Ewins describe an approach to analyze harmonic vibrations of systems with friction interfaces with a developed contact element to evaluate friction forces under a variable normal load and unilateral interaction on the contact interface [8]. The contact elements are derived analytically which allows convergence difficulties due to changes in contact conditions to be overcome. The contact element describes the interaction of surfaces at one node which can be applied to many nodes and describe complex areas. This contact element is applied to an industrial turbine blade model with friction dampers; figure 2.7 shows the finite element model. The effectiveness of the element is demonstrated in the practical application in predicting the contact forces as well as predicted damping and vibration amplitude. The authors also found significant levels of super-harmonic resonances caused by friction when the contact surfaces partially separated.

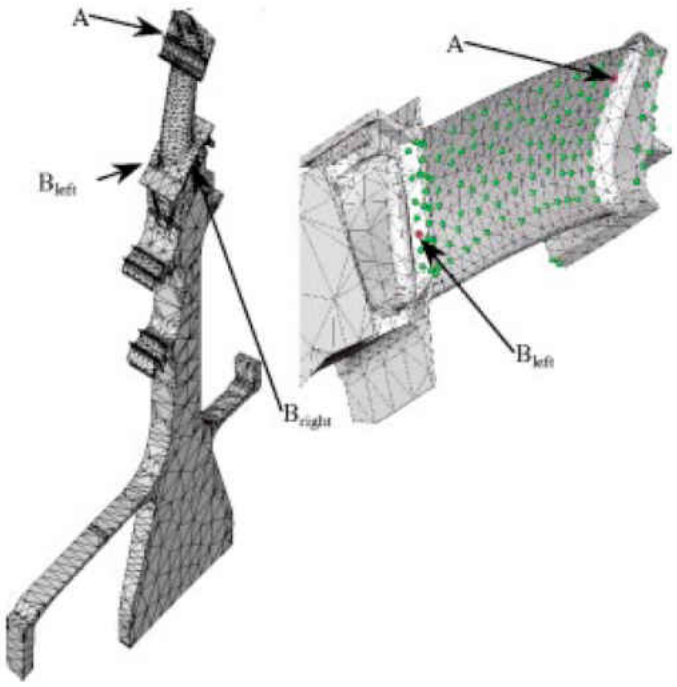

Figure 2.7: Realisitc Turbine Blade Model. From [8]

Deshmuhk et al. investigate the convergence behavior of a contact element for physical parameters such as the system response amplitude and friction state [26]. The contact element used by the authors is an Iwan-type with a multipoint contact microslip model. The results demonstrate that the kinematic behavior of the interface converges slower then the system response which is why contact interfaces need a higher order model to capture the behavior. The results also point out a magnitude dependence on the number of elements needed to achieve model order independence in the forced response prediction to assist in model reduction method development. However the results presented here are using simple linearized models for an academic investigation but still provide valuable insight into the model development and model reduction strategies.

While there are numerous methods availible for the nonlinear analysis of turbine blades with friction dampers they require a good understanding of the input parameters and model generation for reliable predictions. Petrov discusses a method to calculate the forced response based on the contact interface parameters such as the friction coefficient and contact stiffnesses [27]. This is made possible through a derivation of the sensitivities of the harmonic forces with respect to variations in the contact parameters. This method is then applied to an industrial bladed disk with friction contacts to analyze the influence of variations in the contact parameters on the predicted forced response of the system. The full finite element model of the industry blade was reduced down to one sector through the use of cyclic symmetry to be able to account for the nonlinear vibrations. This method allows the optimal contact parameters of the friction dampers to be chosen for design to provide the minimum forced response levels.

Petrov presents a model reduction method for the analysis of the nonlinear forced response of structures with contact interfaces [1]. The method creates a modification to the frequency response function (FRF) matrix to create a more simpler version. This allows a more accurate FRF matrix and reduces models to much less degrees of freedom then possible by other methods while maintaining accuracy of the forced response. This method is applied to the nonlinear forced response of turbine blades with friction contacts such as blade roots and underplatform dampers. For the case of a bladed disk with underplatform wedge dampers, the proposed method is shown to be invariant to the number of retained modes in the predicted forced response, whereas conventional modal models are influenced by the number of retained modes; figure 2.8 shows this comparison. This method offers a new moddeling technique which provides accurate forced response prediction

of bladed disks without the need for as many mode shapes in the analysis. This leads to reduced computation time of the forced response and corresponding modal analysis.

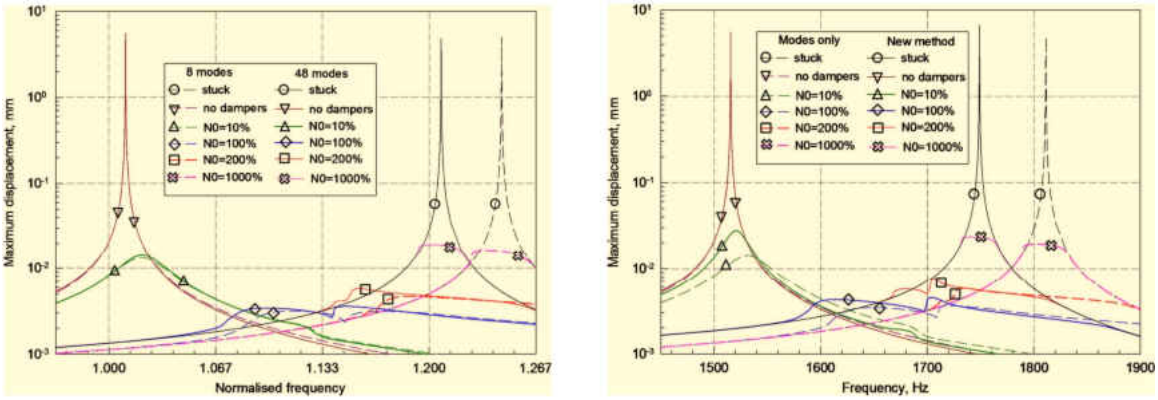

Figure 2.8: Forced Response Results with Old and New Method. From [1]

Schwingshackl et al. investigate the effect of contact interface parameters have on the predicted vibration characteristics of turbine blade coupled with underplatform dampers [28]. The authors focus on improving the modeling techniques of the nonlinear behavior associated with friction at the contact interfaces between blades and dampers. The predicted response of blade and damper systems are rather sensitive to their input parameters and these parameters themselves have uncertainty with their values. The authors also investigate the influence the number of modes retained with the damper had little influence on the response to this specific configuration. The results of the investigation revealed that the tangential contact stiffness, friction coefficient, static normal load, mesh density and placement have the most influence on the predicted forced response of this specific system where wedge underplatform dampers were used. Following these results, the authors investigated the three contact interface parameters mentioned previously to compare measured and estimated values and their effects on the predicted response [29]. The work compares

the reliability in measuring the friction coefficient, tangential contact stiffness and normal load distribution with a comparison between simulated and experimental results of the frequency response. The authors describe a test rig developed to measure the friction coefficient and tangential stiffness between two surfaces. The test rig was demonstrated to reliable and robust in terms of measuring the contact parameters between two surfaces. Additionally a finite element model of the test rig was created to validate the measurement and analysis procedure, where the friction and tangential contact stiffness terms were able to be reliably extracted to replicate the behavior of the test rig. The results of the investigation revealed that if the contact parameters of the interfaces are unable to be accurately measured, the average values of the contact parameters with a temperature dependent friction coefficient can be used for input. This verifies the use of estimated values for the contact parameters used in the prediction of friction contact.

There are a vast amount of methods that have been developed in order to describe the contact dynamics and model reduction in the analysis of the forced response of blades. These methods range from building up from academic examples to building models to match results seen in experiments using industry blades. The academic methods which show promise still need to be verified and tested using more complex blade models and systems which are common in industrial application. In addition the results presented within the friction damping/forced vibration response community are all with respect to a different blade model or system which makes the comparison of the results difficult. There still remains a relatively large gap between academic and industry in terms of application in predicting the forced vibration response of blades. The blade models presented in the following sections aim to be candidates for further academic analysis where the

numerous methods can be used to compare results with a standard blade geometry. These blade models also serve as a medium to help bridge the gap between academic and industrial application because the blades are relatively simple in terms of their physical descriptions but behave qualitatively similar to industrial blades with respect to convergence behavior and sensitivities to friction contact parameters.

CHAPTER 3
BLADE/DAMPER SETUP AND CONSTRUCTION

3.1 Introduction

The goal is to present two blade geometries coupled with underplatform dampers to act as a basis of comparison for predicting the forced vibration response of turbine blades. The geometry of the blades are intended to be as simple, yet complex to capture behavior seen in the forced response of high-fidelity blade models used in industry. The simple design of the blades is to allow for easy implementation into alternative methods developed in predicting the forced vibration response of turbine blades. This section is organized as follows, first the coordinate system and variables used to describe the geometry of the blade designs along with the mathematical constraints are discussed. Then the implementation of designing the first blade and its corresponding damper are discussed followed by the second blade and damper.

3.2 Setting up blade coordinate systems, constraints

First the blades are described in a 2D coordinate system, shown in figure 3.1. The profile of the blade is then labeled with points used to define the model. These points encompass the boundaries

of the model and serve as reference points for the following construction of the 3D model. The coordinate system used in figure 1 is located at the center of rotation, that is, at the center of the disk assembly the blades attach to with the z-axis being the engine axis. This coordinate system is later referred to as the global coordinate system of the blade. The blade itself is centered along the y-axis of this coordinate system. The points which define the boundaries of the blade design here are labeled 0-4 (where $R_0 - R_4$ represent the radial dimensions associated with each corresponding point) and are defined in terms of their coordinates, shown in table 3.1.

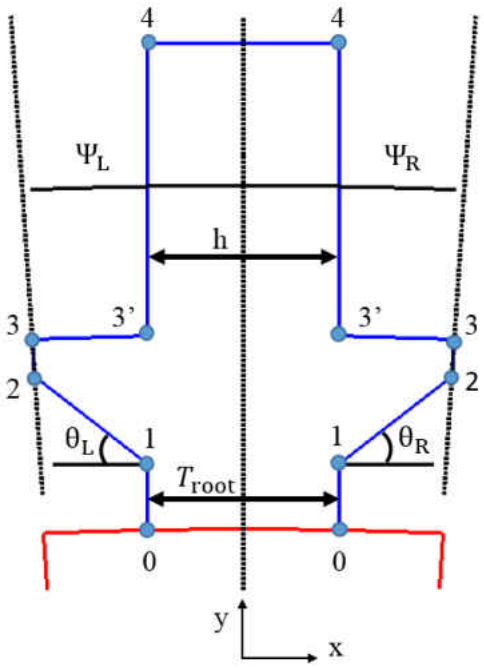

Figure 3.1: Generalized Blade Model

Table 3.1: Coordinates of key points

Point	Left (x,y)	Right (x,y)
0	$(-\frac{T_{root}}{2}, \sqrt{R_0^2 - (\frac{T_{root}}{2})^2})$	$(\frac{T_{root}}{2}, \sqrt{R_0^2 - (\frac{T_{root}}{2})^2})$
1	$(-\frac{T_{root}}{2}, \sqrt{R_1^2 - (\frac{T_{root}}{2})^2})$	$(\frac{T_{root}}{2}, \sqrt{R_1^2 - (\frac{T_{root}}{2})^2})$
2	$(-R_2\sin(\Psi_L), R_2\cos(\Psi_L))$	$(R_2\sin(\Psi_R), R_2\cos(\Psi_R))$
3	$(-R_3\sin(\Psi_L), R_3\cos(\Psi_L))$	$(R_3\sin(\Psi_R), R_3\cos(\Psi_R))$
3'	$(-\frac{h}{2}, \sqrt{R_3^2 - (\frac{h}{2})^2})$	$(\frac{h}{2}, \sqrt{R_3^2 - (\frac{h}{2})^2})$
4	$(-\frac{h}{2}, \sqrt{R_4^2 - (\frac{h}{2})^2})$	$(\frac{h}{2}, \sqrt{R_4^2 - (\frac{h}{2})^2})$

The constraints on the design of the blade are defined next. The total area which a turbine blade is constructed in is refereed to as the blade sector. The value of the blade sector is a function of the number of blades (N), which are evenly spaced around the disk, so each blade may encompass an arc based on the total arc of a circle (360°) divided by the number of blades. For example if there are 45 blades placed evenly around the disk, then each blade may encompass a total arc of 8°. Referencing figure 3.1, the lines connecting points 1 & 2 are at a constant angle relative to the horizontal and represent the platform angles (θ_L, θ_R). Equation 1 ensures that underplatform on the left side of the blade is held at an angle of θ_L. Equation 2 ensures the underplatform on the right side remains at a constant angle of θ_R. Equation 3 represents the total sector angle the blade may encompass with some clearance between adjacent blades (denoted χ). Equation 4 is a constraint on the distance between points 2 and 3 to ensure the thickness of the platform on either

side is the same (denoted PT). The constraint equations (equations 3.1-3.4) are written in terms of the variables from figure 3.1.

$$\tan(\theta_R) = \frac{y_{2R} - y_{1R}}{x_{2R} - x_{1R}} \tag{3.1}$$

$$\tan(\theta_L) = \frac{y_{2L} - y_{1L}}{x_{2L} - x_{1L}} \tag{3.2}$$

$$\Psi_L + \Psi_R = \frac{360^\circ}{N} - \chi \tag{3.3}$$

$$R_3 - R_2 = PT \tag{3.4}$$

Some of the dimensions and constraints mentioned previously were chosen based on experience with realistic blade designs. The values of R_0 and R_4 (representing the blade base and blade tip) are chosen first to constrain the upper and lower bounds of the blade design. Then the platform angles (θ_L & θ_R) were chosen. The blade root thickness (T_{root}), number of blades and radial heights of the blade ($R_0 - R_4$) were chosen based on the respective realistic blade of interest. For both of the blades, the gap between adjacent blades (χ) was chosen to be 10° and the platform thickness (PT) as 10 mm these values were chosen base on previous experience with industrial blade models. The dimensions used to design the blades were picked from a family of industrial turbine blades and modified as needed to produce the desired behavior in the academic blades.

The equations constraining the design of the blade defined earlier (equations 3.1-3.4) are now rewritten in terms of the coordinates in table 3.1, with all the terms on one side of the equations for input in a non-linear equation solver. The rewritten equations are shown below (equations 3.5-3.8). From these equations there are four unknowns (R_2, R_3, Ψ_L, Ψ_R) with four equations. The solution of this system of nonlinear equations will generate the rest of the dimensions needed to generate the blade model based on geometrical constraints outline earlier. The equations were solved using MATLAB's fsolve command which employs a trust-region-dogleg algorithm.

$$R_2[\sin(\Psi_R)\tan(\theta_R) - \cos(\Psi_R)] - \frac{h}{2}\tan(\theta_R) + \sqrt{R_1^2 - (\frac{h}{2})^2} = 0 \tag{3.5}$$

$$R_2[\sin(\Psi_L)\tan(\theta_L) - \cos(\Psi_L)] - \frac{h}{2}\tan(\theta_L) + \sqrt{R_1^2 - (\frac{h}{2})^2} = 0 \tag{3.6}$$

$$\Psi_L + \Psi_R + 0.05^\circ - \frac{360^\circ}{N} = 0 \tag{3.7}$$

$$R_3 - R_2 - 10 = 0 \tag{3.8}$$

The blade models used in predicting the forced vibration response use cyclic expansion, which assumes that the blade model is symmetric for the N bladed disk assembly and therefore only one blade section of the system needs to be modeled. The bladed disk assembly is assumed to be tuned, this assumes that the blades are all identical with respect to their geometry, and dynamic properties such as natural frequencies and mode shapes. However, only the blade is of interest and the mass-

less disk is merely used for the cyclic expansion of the model during the forced response prediction. The root of the blade is assumed to be fixed where the blade would attach to the disk. The blades are excited using a point load on the leading edge blade tip, which is the force later varied in the forced response calculation. Whereas the industrial blades are excited with a full pressure load; this simplification of using a point load was tested on industry blades. Both the point load and full pressure loads produced similar forced response results, at least when the magnitude of the point load was scaled to an appropriate level, this is shown and discussed further in the results section. The material for the blades and associated underplatform dampers were chosen to be steel, which is representative of materials used in gas turbines. Each of the blades presented here is coupled with an associated underplatform damper, with a general overview given next.

3.2.1 Underplatform Damper Setup

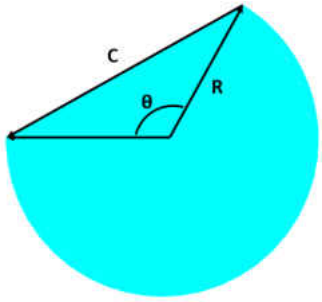

Figure 3.2: Academic Damper

The underplatform dampers are asymmetrical type, with a flat contact on one side and a curved contact surface on the other. Figure 3.2 displays a general drawing of an asymmetrical damper with dimensions used to define the damper design. The force from the damper on the blade platforms

is assumed to be constant and due to centrifugal force. It should be noted that the orientation of the damper during operation is not necessarily matched with what is shown in the figures. During operation, the damper will rotate such that the entire flat face will be in contact with the under-platform of the blade. The dimensions for the dampers were scaled from dimensions of realistic dampers. The ratio of the length of the flat face of the damper (denoted C) to the radius (R) was used as a parameter in the design of the academic dampers, constraining the relationship between C and R is equivalent to constraining the angle subtended by the chord length (C). To be clear the chord length C and chord angle θ refer to the chord of the circle in the damper cross-section; they are different then the airfoil chord. This ratio was maintained in the designed dimensions of the academic dampers with their respective realistic counterparts.

The formulation of the area of the academic dampers is described next. To maintain the ratio between the radius and chord lengths, the new values must both be scaled by the same amount. The area of the asymmetrical damper can be thought of as the area of a full circle (given by πR^2), minus a sector area (given by $\pi R^2 \frac{\theta}{360^\circ}$), plus the area of the triangular shape (given by $\frac{1}{2}CR\cos(\frac{\theta}{2})$), which is shown below in equation 3.9. The value of θ is kept constant.

$$A = \pi R^2 - \pi R^2 \frac{\theta}{360^\circ} + \frac{1}{2}CR\cos(\frac{\theta}{2}) \tag{3.9}$$

To maintain the ratio between the radius and chord lengths, the new values must both be scaled by the same amount. This value written in terms of a variable γ. This variable represents the value the radius and chord dimensions of the academic damper will be scaled, represented below in equation 3.10, where R represents the original radius and $\overline{R}$ is the scaled up radius.

$$\overline{R} = \gamma R, \overline{C} = \gamma C \tag{3.10}$$

The value of of the scaling parameter (γ) was chosen based off a damper mass parameter study and examining the resulting damping-amplitude response curves of the system. Based on the results of the damper mass variation using DATAR, a scaling factor for the mass is chosen when the response of the damping curves begin to display diminishing returns. Since the scaling factor affects the mass of the damper, the volume of the damper needs to be scaled the same amount to keep the ratio, in order to maintain the density value the same (that of steel). Using the relations in equation 3.10 and equation 3.9, the relationship between the original damper cross-sectional area and scaled up area is derived below. The length of the damper is fixed and based off of the respective industry counterpart.

$$\overline{A} = \pi\overline{R}^2 - \pi\overline{R}^2\frac{\theta}{360^\circ} + \frac{1}{2}\overline{CR}\cos(\frac{\theta}{2}) \tag{3.11}$$

Using the relation above in equation 3.10.

$$\overline{A} = \pi R^2\gamma^2 - \pi R^2\gamma^2\frac{\theta}{360^\circ} + \frac{1}{2}C\gamma R\gamma\cos(\frac{\theta}{2}) \tag{3.12}$$

$$\overline{A} = \gamma^2(\pi R^2 - \pi R^2\frac{\theta}{360^\circ} + \frac{1}{2}CR\cos(\frac{\theta}{2})) \tag{3.13}$$

$$\overline{A} = \gamma^2 A \tag{3.14}$$

From the relation above in equation 3.14, the value of γ^2 is set equal to the scale factor which the academic damper will be when compared to its industry counterpart. The mass of the damper was chosen by conducting a damper mass variation in DATAR using a generic damper. The resulting forced response curves were examined and the value of the scaled mass was chosen based on when diminishing returns were visible in the damping-amplitude response curves. With the material of the damper already chosen (steel), the scale factor was calculated to mach material density and representative mass.

The underplatform dampers discussed in the following sections are representative of physical specimens, however the forced vibration response results and models are purely numerical. The academic dampers discussed in the models are rather large in size and mass compared to dampers seen in industry. One reason for this is that the academic blades geometries are rather large themselves due to the blades being solid. Industry blades are commonly hollow which would alleviate the issue of need a larger damper, but a solid blade was kept in interest of academic simplicity. Additionally, industry blades have more complex shapes in the blade design which allows more vibration of the blade to be transmitted to the underplatform region of the blade, leading to more relative motion between the damper and platform, causing more friction and energy dissipation. A better coupling of the blade motion to the underplatform region of the academic geometries would also alleviate the need for a large underplatform damper as well.

The friction contact model used by DATAR incorporates the surface roughness of the contact interface to model the contact dynamics. DATAR allows inputs of the surface roughness of the blade platform and damper surfaces and calculates an effective surface roughness based on these

values. In the parametric studies conducted later, the platform surface roughness is kept constant while the damper surface roughness is varied. The baseline values used for the damper roughness are provided in their respective tables which are discussed later.

3.3 Academic Geometry 1

This section describes in detail the procedure followed in the design of the first academic blade geometry and its associated damper. First, values for $R_0, R_4, \theta_L, \theta_R, N$, and T_{root} were chosen to be representative of a realistic turbine blade. The other dimensions of the blade (R_2, R_3, ψ_L, ψ_R) were generated by solving the four nonlinear system of equations (equations 3.5-3.8) discussed previously. The 3D blade models were generated using ANSYS Mechanical APDL, there is an input file included in the appendix which can be run in ANSYS APDL to generate the blade model shown here. However, the methodology described here should be able to be implemented in any available CAD software. This section is organized into three parts, the first describes the blade platform, the second describes the design of the blade section above the platform and the last describes the underplatform damper design.

3.3.1 Platform

The driving factor in the geometry of the platform region of the blade model is the underplatform angles (θ_L, θ_R) and the distance from the platform base (R_0) to the underplatform neck (R_1). When

the underplatform angles are not equal ($\theta_L \neq \theta_R$) as in this case, there are a multitude of approaches to construct the platform area. In this instance, based on realistic blade designs, the radial heights of the blade were kept constant on both sides of the platform. The result creates different platform lengths on either side of the blade; figure 3.3 demonstrates this. Using the coordinates described earlier in table 3.1, the key point command in ANSYS was used to create the points (0-4) by substituting the dimensions for the first blade using the Cartesian coordinate system shown earlier in figure 3.1. These points were then connected with lines and arcs to create a closed 2D geometrical sketch; figure 3.3 shows the result. The lines connecting points 0-1, 1-2, and 3-2 are straight lines while the lines connecting 0-0, and 3-3' are arcs centered about the Cartesian (global) coordinate system. This area was then extruded by the length of the blade model noted in table 3.2 or 300 mm in this case; figure 3.5 shows the resulting 3D blade model. The design of the blade model above the platform is discussed next.

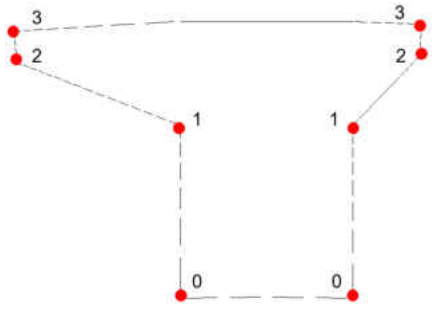

Figure 3.3: Sketch of Platform

3.3.2 Blade

The blade profile (section of blade model from points 3' to 4 in figure 3.1) design (region above the platform) was conducted by implementing a modal analysis of the blade model and comparing with the results from a realistic blade. Initially the blade thickness (h) and root thickness (T_{root}) were set equal and varied to find a value that would allow the first bending mode frequency to match that of the realistic blade. The results demonstrated that the required thickness was too large to hit the desired frequency and a more complex blade profile was needed; figure 3.4a shows an example of the blade thickness required to reach the targeted frequency.

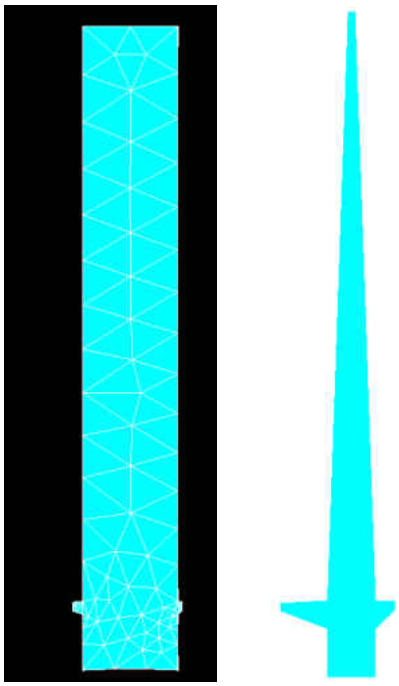

(a) Thick Blade (b) Taper

Figure 3.4: Blade Profile Design Iterations

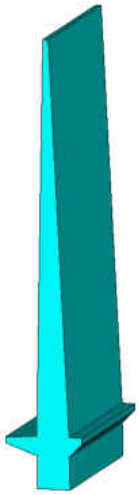

Figure 3.5: Academic Blade Geometry 1 Model

To keep the design as simple as possible a linear taper was added to the blade profile to hit the targeted first bending frequency. The linear taper along the blade allowed the blade thickness to remain close to realistic blades and hit the targeted frequency while keeping the design simple. The decision to implement a taper on the blade profile over more realistic complexity (such as curvature along the blade and a hollow blade) was to keep the blade model simplistic for academic implementation while still reaching the desired first bending frequency. The linear taper was implemented on the blade profile by only adjusting the blade tip thickness; figure 3.4b shows the resulting taper implemented. The thickness of the blade profile (h) at the platform or base of the blade profile is equal to the root thickness (T_{root}), while the blade profile thickness at the tip of the blade was set to the value of 8.33 shown in table 3.2. The blade model was then extruded into 3D a distance of 300 mm; figure 3.5 shows the resulting 3D model of the blade design, table 3.2 lists the dimensions and properties of the blade model.

Table 3.2: Academic Geometry 1 Properties

Number of Blades (N)		45
Broach Angle	[°]	0
Underplatform Surface Angles (θ_L/θ_R)	[°]	25/50
Disk Radius (R_0)	[mm]	850
Underplatform Neck Height (R_1)	[mm]	905
Underplatform Height (R_2)	[mm]	928
Platform Height (R_3)	[mm]	938
Blade Tip Height (R_4)	[mm]	1600
Blade Root Thickness T_{root}	[mm]	50
Blade Section Depth	[mm]	300
Blade Base Thickness (h at R_1)	[mm]	50
Blade Tip Thickness (h at R_4)	[mm]	8.33
Blade Density	[kg/m^2]	8000
Blade Modulus	[GPa]	200
Blade Poisson Ratio		0.25
First Bending Natural Frequency	[Hz]	110
Point Load on LE Tip Transverse to Blade	[N]	100

3.3.3 Underplatform Damper

The underplatform damper associated with the first academic blade geometry is of the asymmetrical type with dimensions based off of dampers used in industry. The damper dimensions (R, θ, C, Length) were chosen using the procedure mentioned previously in the underplatform damper setup section and will be briefly mentioned here. First a generic damper was used to conduct a damper mass sensitivity study with respect to damping on the forced response using the academic blade geometry. The results of the study indicated the scale factor to be used on the dimensions of the realistic damper to generate the academic damper. The finite element model of the damper was then created in ANSYS Mechanical APDL; table 3.3 lists the dimensions and properties of the first academic underplatform damper, figure 3.6 shows the finite element model of the damper.

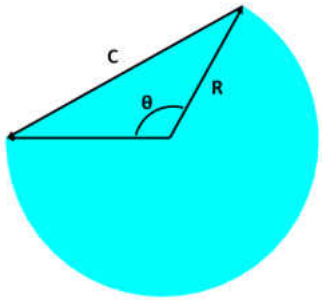

Figure 3.6: Academic Damper 1

Table 3.3: Academic Damper 1 Properties

Radius (R)	[mm]	17.5
Chord Length (C)	[mm]	30.31
Chord Angle (θ)	[$^\circ$]	120
Damper Length	[mm]	300
Density	[kg/m^2]	8000
Mass	[kg]	1.89
Damper Roughness	[nm]	15
Friction Coefficient		0.33

3.4 Academic Blade Geometry 2

This section describes the procedure followed in the design of the second blade geometry and associated underplatform damper. The blade geometry described here has many differences from the first blade geometry. The blade profile above the platform is much smaller then the first (about 700 mm vs 400 mm). A broach angle is incorporated into the design and the platform angles are symmetric, whereas the first blade had no broach angle and non-symmetric platform angles.

First, the values for $R_0, R_4, \theta_L, \theta_R, N$, and T_{root} were chosen to be representative of a real turbine blade. The rest of the dimensions (R_2, R_3, ψ_L, ψ_R) were generated by solving the nonlinear system

of equations (equations 3.5-3.8) defined previously. As with the first geometry, this blade was modeled using ANSYS Mechanical APDL and an input file is included in the appendix which can be used in ANSYS to generate the blade model.

The second blade geometry adds another layer of complexity with the incorporation of a broach angle. To keep the design relatively simple, the construction of the blade model was separated into two parts (platform and blade profile) and later merged together. The procedure in which the platform was constructed in ANSYS is discussed next, followed by the blade profile and then the underplatform damper.

3.4.1 Platform

The platform design is more involved with the incorporation of a broach angle in the blade model. This is because the disk section which the blade attaches to can be thought of as a cylinder. The blade model in 3D needs to conform to the profile of the disk, with virtually no gap between the base of the blade root and the disk section. The design of the platform needs to maintain conformity with the disk during the extrusion of the model into 3D. That is, the platform is extruded along the edge of a cylinder which is representative of the disk. First the key points of the platform profile were created in the global *x*-*y* coordinate frame using the dimensions for $R_0 - R_3$; which are given in table 3.4. These key points were then connected with lines and an area was generated from the lines;3.7a shows this resulting platform.

The platform was then extruded into 3D using a cylindrical coordinate system with the VEXT command. The VEXT command allows control of an extrusion in all coordinate directions independently (r, θ, z). The value of the extrusion in the radial direction (r) is zero because the radial dimensions of the platform are not changing during the extrusion. The value of θ, or the amount of rotation the extrusion will experience being extruded along the disk is governed by equation 3.15 and has a value of 3.8°. Where L represents the length of the extrusion in the rotated frame. The length of the extrusion (L) in the global frame (z) is defined in equation 3.16 and has a value of 193.2 mm.

$$\theta = \frac{L\tan(15^\circ)}{R_0} \tag{3.15}$$

$$z = L\cos(15^\circ) \tag{3.16}$$

This is done to ensure conformity with the outside edge of the disk section; figure 3.7b shows the cylindrical coordinate system used in the extrusion and the result. Figure 3.7c shows the platform using the VEXT extrusion on the disk section which is on the bottom of the picture. This approach ensures that when the blade model is expanded into N blades, the platform will form a shell, minus the gap of 0.05°.

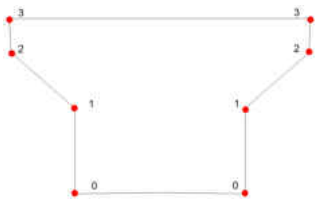

(a) Platform Area

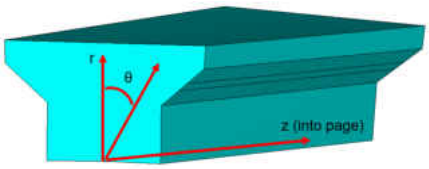

(b) Platform Extrusion with Coordinate System

(c) Platform Extrusion with Disk

Figure 3.7: Academic Geometry Platform Constuction

During the design of the platform region, multiple methods were investigated to construct the model such that the blade root would properly conform to the disk. The chosen method discussed previously is a hybrid of two other methods investigated in the construction of the blade platform. The first alternative method involved sketching the entire blade model (platform and blade profile) in the rotated broach frame and then conducting a linear extrusion; figure 3.8a shows the resulting extrusion with the disk modeled. This method leaves some space between the blade root and disk which can be seen in figure 3.8a and would need to be filled in. Additionally, there is extra blade material which would need to be cut from this extrusion in order to make the leading edge and trailing edge of the blade parallel to the global x-axis. The other method involved extruding the entire blade sketch along a curve representing the outside edge of the disk; figure 3.9a shows the result of this. While this method does produce good conformity with the disk, there is an associated

twist with the blade section that is unwanted which figure 3.9b shows. From these methods a hybrid of these two methods was created using the VEXT command that was described earlier; figure 3.7c shows the result.

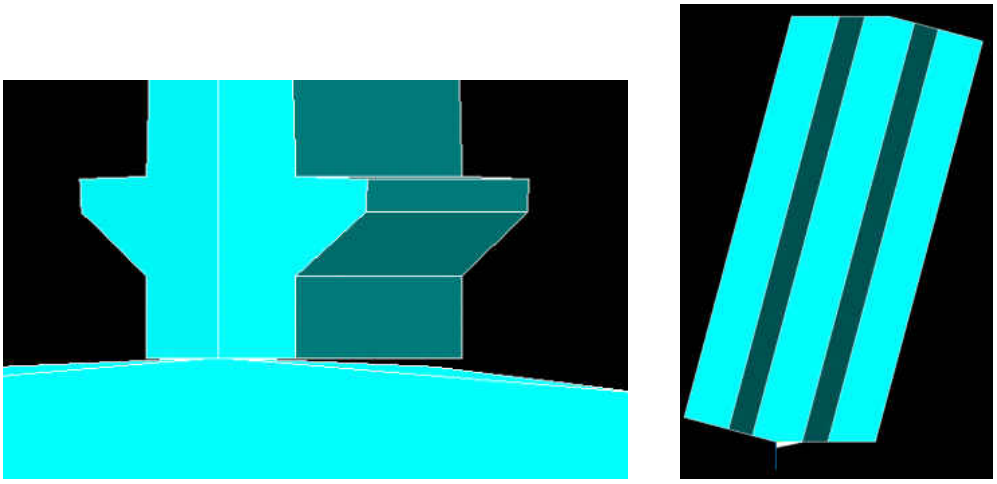

(a) Platform View with Disk (b) Blade View

Figure 3.8: Alternative Method 1 for Platform Construction

(a) Platform Extrusion with Disk from (b) Blade View

Figure 3.9: Alternative Method 2 for Platform Construction

3.4.2 Blade

The construction of the blade profile is not as involved as the platform section. The initial sketch of the blade profile was done in the rotated broach frame (15° rotated from the global coordinate system about y) using the coordinates of points 3' and 4 in table 3.1. The global coordinate system is referring the the coordinate system shown in 3.1, the broach frame is rotated about the y-axis from the global; figure 3.10 shows the broach frame (red) in relation to the global (black). To be clear the coordinate system shown in black here is the same as the global system described in figure 3.1. However, since the blade is sketched and extruded in the broach frame, and the platform was created in the global coordinate system, the blade profile extrusion into 3D needs to be offset from the origin to ensure the blade profile remains on the platform; figure 3.10 shows a top view of the blade model with the offset of the blade profile.

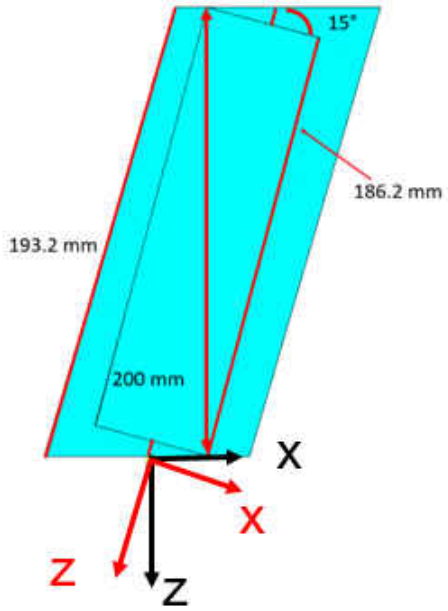

Figure 3.10: Academic Geometry 2 Top View of Blade with Broach Frame (Red)

A modal analysis was conducted on the blade model to determine the thickness and profile of the blade to reach the desired first bending frequency. First only the thickness of the blade profile itself was varied to achieve the desired bending frequency. It was found that with this geometry, there was no need of a linear taper to achieve the frequency of interest. Figure 3.11 shows the finite element model of the full blade model and table 3.4 lists the dimensions and properties of the blade model.

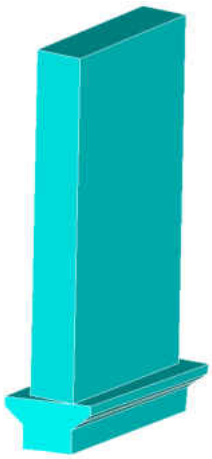

Figure 3.11: Academic Blade Geometry 2 Model

Table 3.4: Academic Geometry 2 Properties

Number of Blades (N)		60
Broach Angle	[°]	15
Underplatform Surface Angles (θ_L/θ_R)	[°]	45/45
Disk Radius (R_0)	[mm]	800
Underplatform Neck Height (R_1)	[mm]	825
Underplatform Height (R_2)	[mm]	842
Platform Height (R_3)	[mm]	852
Blade Tip Height (R_4)	[mm]	1200
Blade Root Thickness T_{root}	[mm]	50
Blade Section Depth	[mm]	200
Blade Base Thickness (h at R_1)	[mm]	50
Blade Tip Thickness (h at R_4)	[mm]	50
Blade Density	[kg/m^2]	8000
Blade Modulus	[GPa]	200
Blade Poisson Ratio		0.25
First Bending Natural Frequency	[Hz]	260
Point Load on LE Tip Transverse to Blade	[N]	100

3.4.3 Underplatform Damper

The associated underplatform damper was designed in the same procedure as the first academic damper are is briefly outlined here. The dimensions (R, θ, C, Length) were chosen to be scaled representative values from realistic dampers. First a generic damper was used to conduct a damper mass sensitivity study to see where the maximum experienced damping began to see diminishing returns. The scaling factor was chosen based on where variations in the damper mass began to experience diminishing returns with a generic damper; figure 3.12 shows the finite element model with dimensions and table 3.5 lists the dimensions and properties of the damper.

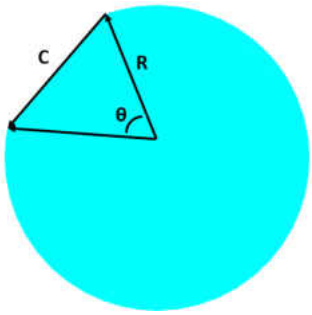

Figure 3.12: Underplatform Damper Model 2

Table 3.5: Academic Damper 2 Properties

Radius (R)	[mm]	20
Chord Length (C)	[mm]	20
Chord Angle (θ)	[$^\circ$]	60
Damper Length	[mm]	200
Density	[kg/mm^2]	8000
Mass	[kg]	1.94
Damper Roughness	[nm]	15
Friction Coefficient		0.33

CHAPTER 4
RESULTS/DISCUSSION

4.1 Introduction

The forced response of the academic blade models were obtained in a process that is outlined as follows. First, a mode-based harmonic analysis of the blade models were conducted using ANSYS Mechanical APDL. The analysis takes a truncated number of modes from the blade finite element model and calculates the eigenvalues, eigenvectors and modal parameters. This was done for only one harmonic index for each respective academic blade models, which was based on the harmonic of interest with respect to the industry blades. The results of the modal analysis were then imported into the nonlinear damping code DATAR.

DATAR calculates the frequency response function of a simulated tuned bladed disk assembly through cyclic expansion of the blade model and combines the modal description of the blade with physical parameters of the contact such as the combined surface roughness (referred to as the damper roughness here) and the friction coefficient. At each value of excitation the frequency response function of the bladed disk assembly using the Harmonic Balance Method across a prescribed frequency range that crosses the first bending frequency of the blade in these cases. The contact force between the blade and underplatform damper is assumed constant and wholly due to

centrifugal force. The friction model used by DATAR is based on Coulomb's dry friction law and assumes a constant coefficient with no influence of temperature and slip velocity.

DATAR is used to vary the excitation force (point load on LE tip for the academic blades which is a modal excitation) of the bladed disk system and calculates the damping, and resonance amplitude given a frequency sweep range. DATAR has the capability to conduct parameter variation studies of a tuned bladed disk assembly as well, the results shown here are parametric plots of the system response based on increasing excitation. In the results presented in the following sections, the inputs into DATAR such as the damper mass, damper surface roughness and friction coefficient are varied to investigate the sensitivities to changes in the forced response of the blade system.

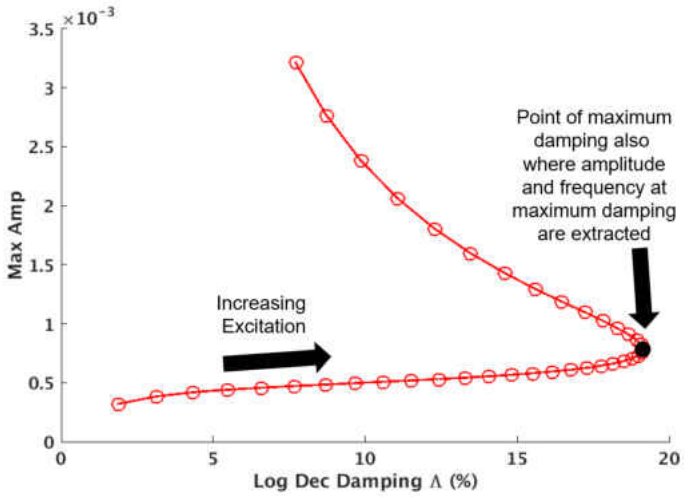

Figure 4.1: Example Forced Response Parametric Plot

The following plots show the calculated damping, vibration amplitude and frequency as a function of increasing excitation. Starting from the bottom left of the plots each point on the curve, moving left to right and up represents an increasing excitation value. At each point of excitation, the damping, amplitude and frequency are calculated with one example shown in figure 4.1.

Figure 4.1 provides a visual representation of the resulting vibration amplitude and damping with increasing excitation as well as pointing out the maximum damping point which is of main interest and will be discussed more later in the results. The vibration characteristics of the blade models are characterized primarily around the point of maximum damping or where the parametric curve begins to turn over on itself. This parametric curve also provides some insight into where the underplatform damper is predicted to be effective and lose effectiveness which is based on the excitation location along the curve. In other words the damper is predicted to be most effective around the point of maximum damping at the turn-over point.

4.2 Validation of Academic Blade Models with Industry Models

This section compares the predicted response of the presented academic blade models with full order realistic blade models, of which the academic blades are representative of. To validate the use of the academic geometries, a behavior observed in the predicted forced response of industry blades known to occur is compared with results using the academic geometries. This behavior occurs when the number of modes in the modal analysis is varied, causing the resulting predicted forced response to change. When the number of retained modes in the modal analysis is increased, the predicted damping decreases, shown in figure 4.2. Figure 4.2 shows the predicted damping and vibration amplitude as a function of increasing forcing excitation when the number of modes are varied in the modal analysis; comparing the industrial and academic blade models.

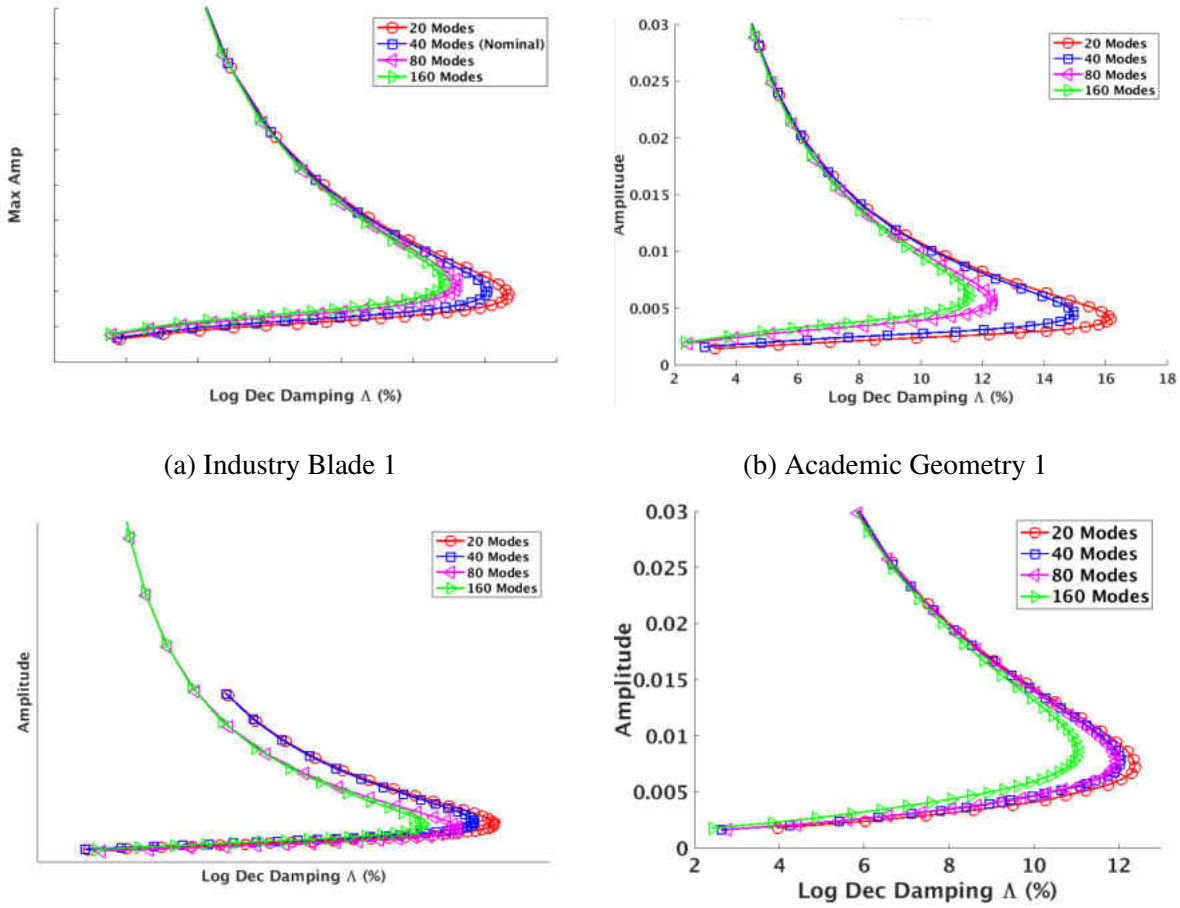

(a) Industry Blade 1

(b) Academic Geometry 1

(c) Industry Blade 2

(d) Academic Geometry 2

Figure 4.2: Forced Response Results Against Modes Retained

From the results in figure 4.2, the predicted forced response of the academic blades match up well with that of the industrial blades. That is, the academic blades behave qualitatively similar to the industrial blades in the forced response prediction when the number of retained modes varies. This is a key behavior seen in the forced response prediction of industrial blade models and was important to replicate with the academic blade models to validate their design. The fact that the simple academic blade models presented here require a large number of retained modes

for convergence is desired since this remains a critical factor in the analysis of high-fidelity blades with reduced order models. The truncated modes in the reduced order models likely introduces an associated numerical stiffness and still remains a question of interest.

The academic blades discussed here are excited using a point load located on the leading edge blade tip, while the industrial blade models are excited using a full pressure load along the entire blade profile. It was mentioned previously that this simplification of using a point load versus a full pressure load produces the same forced response curve when the point load is scaled to an appropriate magnitude. Figure 4.3 compares the response when a full pressure load is used versus a point load and demonstrates that the resulting curve is the same; the same maximum damping and resonance amplitude are reached using both excitation method (the point load however, needs to scaled to the appropriate magnitude to match the excitation caused by the full pressure load). This results demonstrates that the excitation on the blade does not need to be known ahead of time in order to predict the forced vibration response.

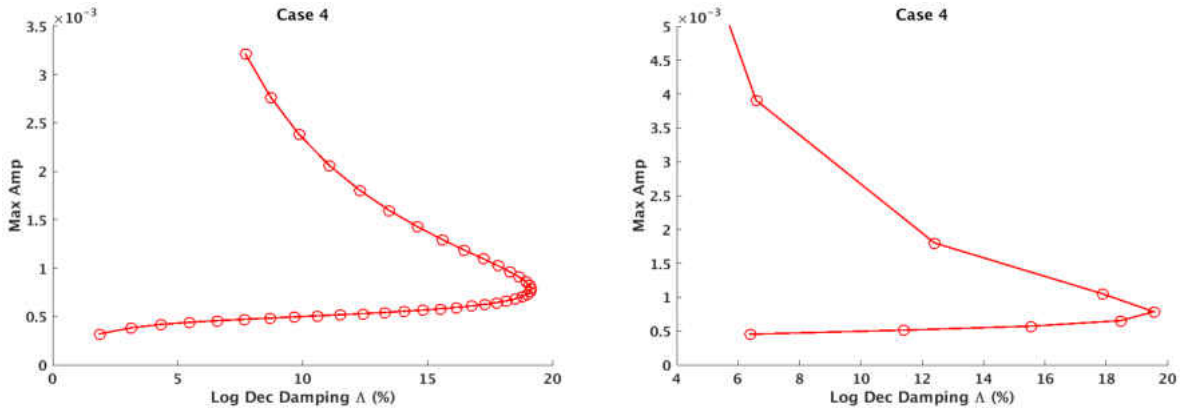

(a) Point Load (b) Full Pressure Load

Figure 4.3: Forced Response Results Comparing Excitation

The results presented in the next section are from the academic blade models and not intended for design purposes; the academic geometries were constructed only to qualitatively match the behavior of the industry blades. The significance of the results is that the proposed academic blades behave qualitatively similar to their industrial counterparts under sensitivities to design parameters; furthermore, they function to provide a point of comparison for alternative forced response prediction methods and candidates for further academic analysis to help bridge the gap between academic and industry application in the forced vibration response community.

4.3 Academic Geometry 1 Results

The nonlinear damping code DATAR was used to vary the excitation force (point load defined in table 3.2) of the blade and conduct variations of design parameters. Figure 4.4 shows how the predicted damping, vibration amplitude and frequency change with respect to changes in the underplatform damper mass, damper surface roughness and friction coefficient as the excitation increases (explained earlier in figure 4.1). The data in figure 4.4 was generated using 40 retained modes in the modal analysis and the trends match behavior seen in industry blades. Figures 4.4a-b show that the predicted damping and amplitude increase with an increase in damper mass. Figures 4.4c-d demonstrate that increasing the surface roughness decreases the predicted damping. Figures 4.4e-f show that increasing the friction coefficient increases the amplitude and slightly decreases the maximum damping.

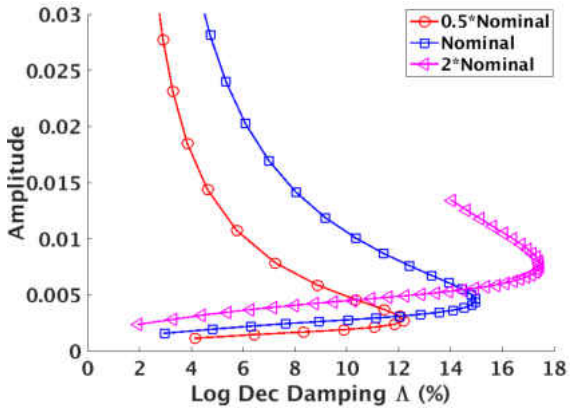

(a) Damp. vs Amp. w.r.t. Damper Mass

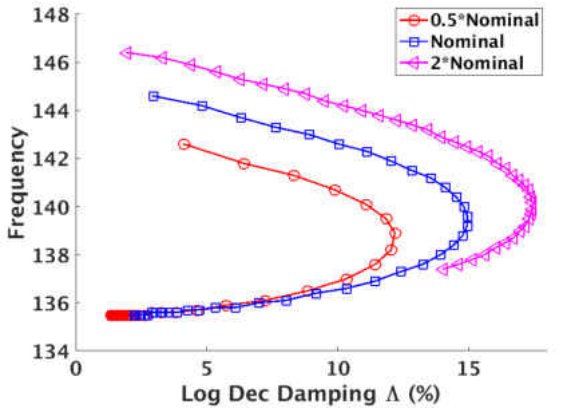

(b) Damp. vs Freq. w.r.t. Damper Mass

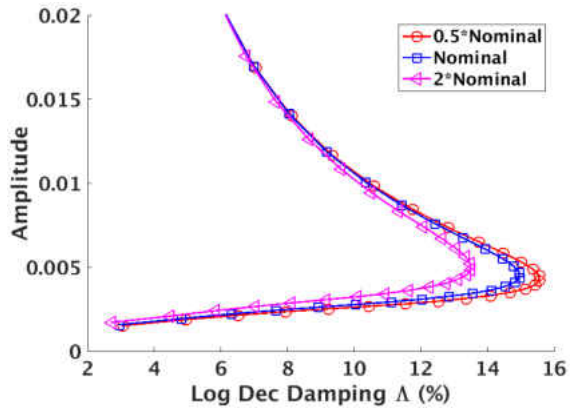

(c) Damp. vs Amp. w.r.t. Roughness

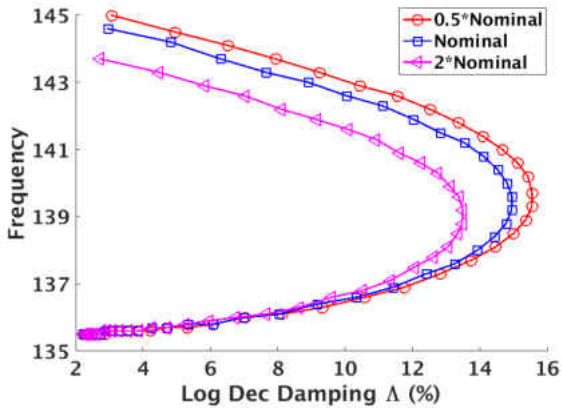

(d) Damp. vs Freq. w.r.t. Roughness

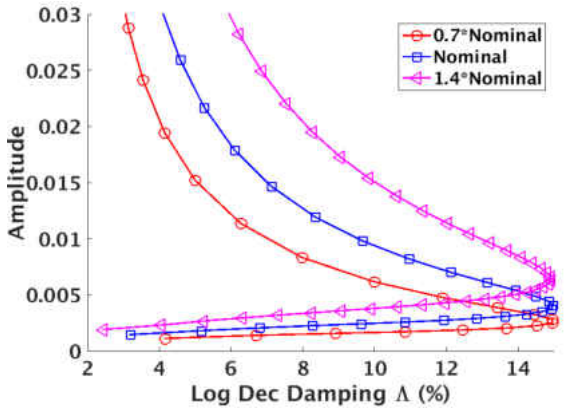

(e) Damp. vs Amp. w.r.t. Friction

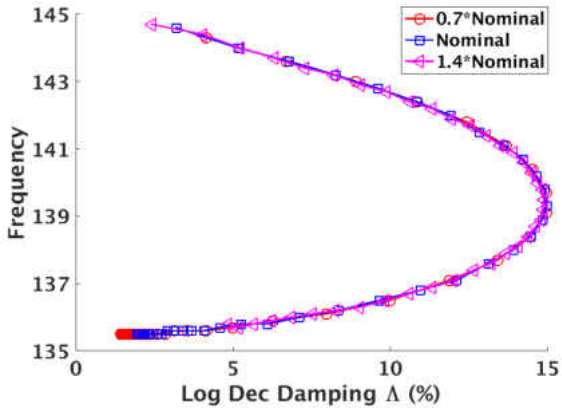

(f) Damp. vs Freq. w.r.t. Friction

Figure 4.4: Academic Geometry 1 Forced Response vs Design Parmater Variations

In addition to the predicted damping and amplitude changing with respect to variations in the design parameters, the excitation (referred to as stimulus) required to reach the maximum point of damping and turn over point also changes. Stimulus refers to the amount the excitation force is increased in percent from its original value (100 N force for the academic blades) which is found in each blades respective property table in chapter 3. The following plots in figure 4.5 show how the excitation changes for the predicted damping and amplitude with respect to variations in the design parameters. The plots show how the variation in the design parameters impact the excitation needed to generate the forced vibration response. Figures 4.5a-b show that as the damper mass increases, the excitation needed to generate the same predicted forced response increases. Figures 4.5c-d show that as the damper roughness has very little effect on the stimulus location of the maximum damping point. Figures 4.5e-f show that the stimulus of the maximum damping point increases with an increase in the friction coefficient in addition to the amplitude increasing.

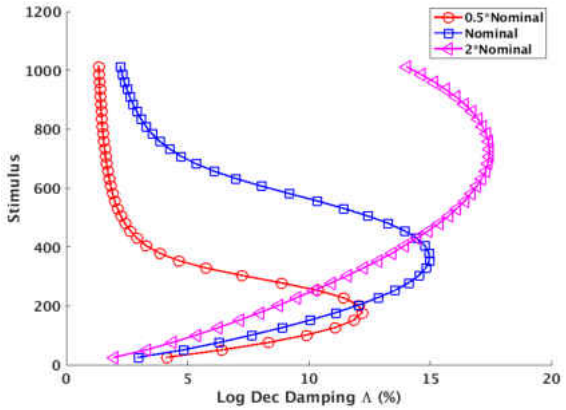

(a) Damping vs Stimulus w.r.t. Damper Mass

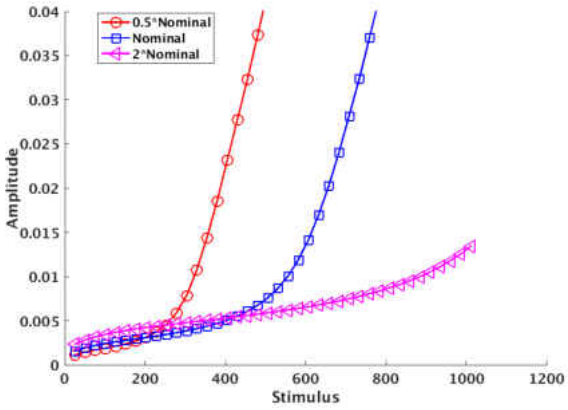

(b) Stimulus vs Amplitude w.r.t. Damper Mass

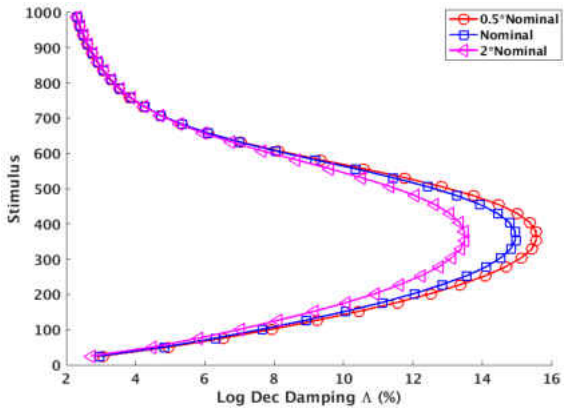

(c) Damp. vs Stim. w.r.t. Damper Roughness

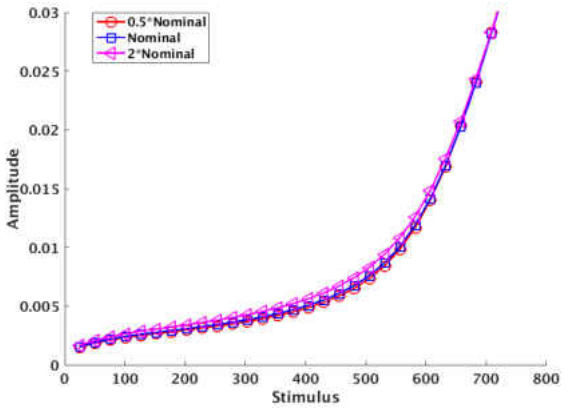

(d) Stim. vs Amp. w.r.t. Damper Roughness

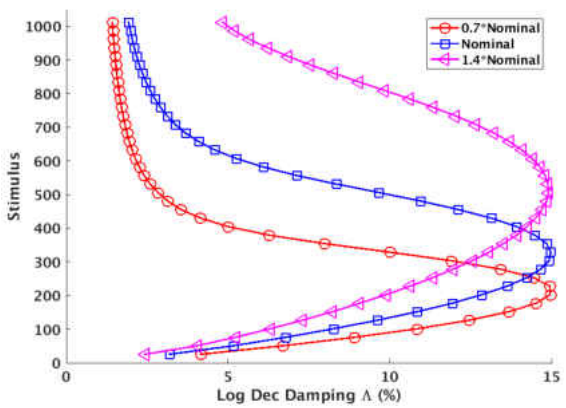

(e) Damping vs Stimulus w.r.t. Friction

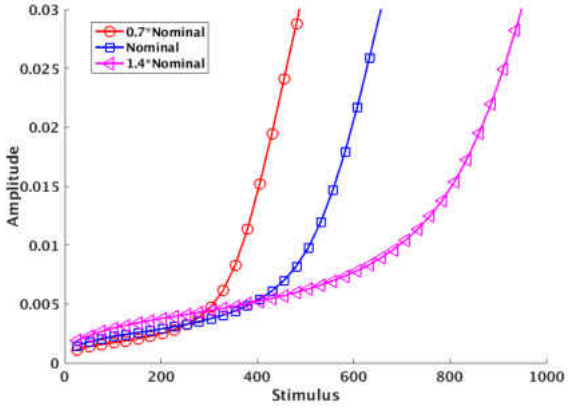

(f) Stimulus vs Amplitude w.r.t. Friction

Figure 4.5: Academic Geometry 1 Excitation vs Design Parmater Variations

The sensitivity of the first academic blade model to the design parameters (damper mass, surface roughness, and friction coefficient) is shown next and is compared between models using a different number of retained modes in the modal analysis. Figure 4.6 shows the sensitivity of the maximum damping, amplitude at maximum damping, frequency at maximum damping to variations in the design parameters. The results are normalized with respect to the nominal parameter value of the calculated damping, amplitude and frequency of the 160 mode reduced order model.

Figures 4.6a-c shows that as the damper mass increases, the maximum damping, amplitude at maximum damping increase, while frequency at maximum damping remains relatively constant. Figures 4.6d-f shows that as the damper surface roughness increases, the maximum damping decreases, while the amplitude at maximum damping increases, and frequency at maximum damping remains relatively unchanged. Figures 4.6g-i shows that as the friction coefficient increases, the maximum damping and frequency at maximum damping remain relatively unchanged, while the amplitude at maximum damping increases.

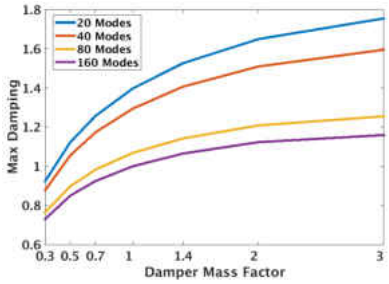

(a) Damping w.r.t. Damper Mass

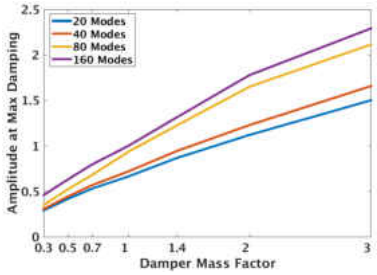

(b) Amp. w.r.t. Damper Mass

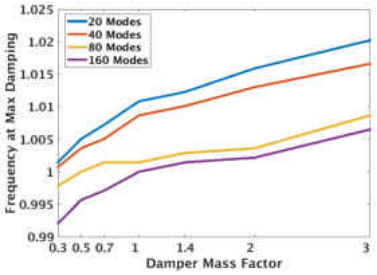

(c) Freq. w.r.t. Damper Mass

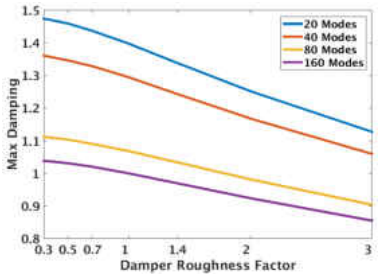

(d) Damping w.r.t. Roughness

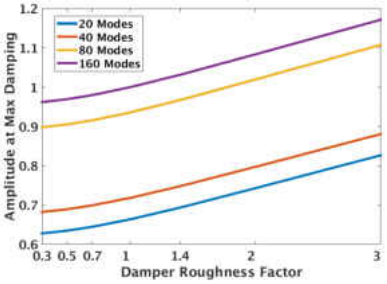

(e) Amplitude w.r.t. Roughness

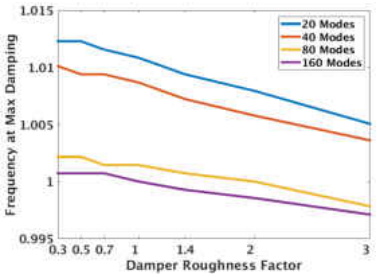

(f) Frequency w.r.t. Roughness

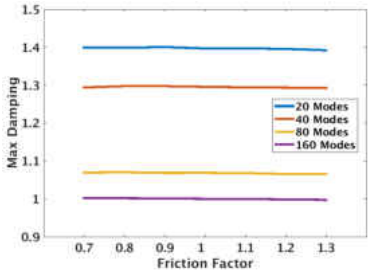

(g) Damping w.r.t. Friction

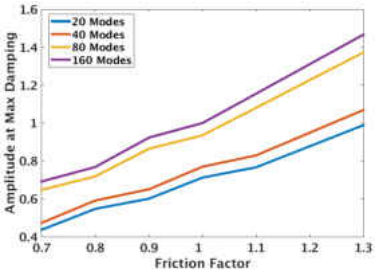

(h) Amplitude w.r.t. Friction

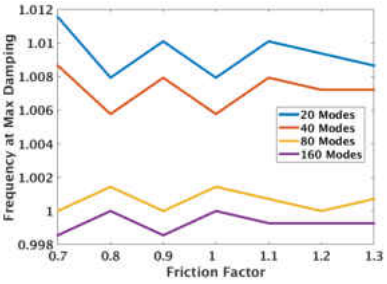

(i) Frequency w.r.t. Friction

Figure 4.6: Sensitivity of Academic Geometry 1 to Design Parameter Variation

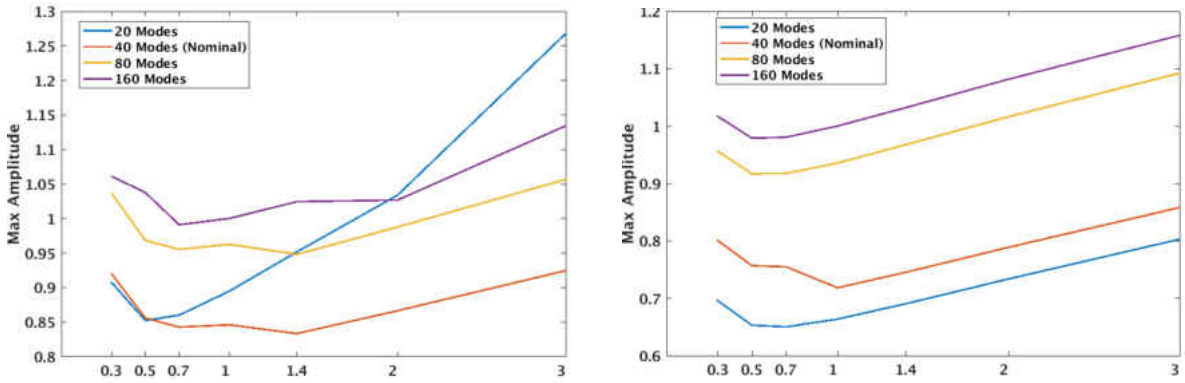

(a) Oscillatory Convergece

(b) Monotonic Convergence

Figure 4.7: Example of Blade Sensitivity Behavior

Early in the vibration response characterization of academic blade geometry 1, the sensitivities of the blade to design parameters did not display monotonic convergence as shown in figure 4.6 but instead oscillatory convergence between the reduced order models; figure 4.7 shows the oscillatory behavior seen and the monotonic convergence after the solution was found. It was thought and later confirmed that this was due to the coarse meshing of the platform region of the blade, particularly the underplatform area where the dampers would make contact with the blade. The mesh of the platform region was therefore increased roughly by an order of magnitude; figure 4.8 shows the initial mesh and more dense mesh of the platform region. The original mesh of the platform region had an element size of approximately 20 mm with the nodes every 10 mm, where the updated mesh has an element size of approximately 10 mm with nodes every 5 mm. The sensitivity studies were then conducted again and the resulting data behaved as expected with monotonic convergence between the reduced order models; figure 4.6 shows these results.

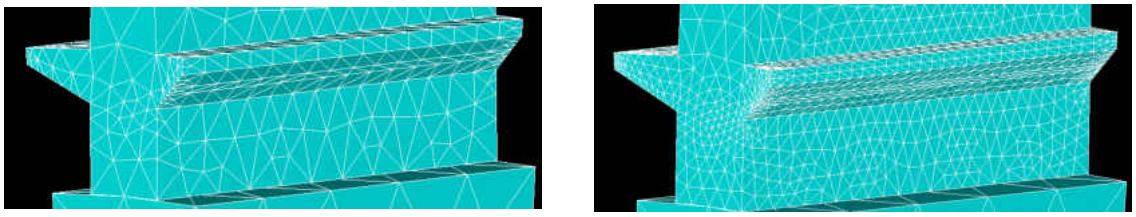

(a) Orignial Platform Mesh

(b) Refined Platform Mesh

Figure 4.8: Comparison of Platform Mesh

4.4 Academic Geometry 2 Results

The results for the second academic blade model are provided next; the blade model was analyzed in the same procedure as the first. Figure 4.9 shows how the predicted response of the blade changes to variations in the damper mass, damper surface roughness and friction coefficient. The results presented here were generated using a 40 mode reduced order model. Figures 4.9a-b shows that as the damper mass increases, the predicted damping, and amplitude increase. Figures 4.9c-d shows that the as the damper surface roughness increases, the predicted damping decrease and the amplitude remains unchanged. Figures 4.9 shows that as the friction coefficient increases, the damping slightly decreases while the amplitude increases. It is worth pointing out that the non-smooth portion in figure 4.9b is due to a rather flat response in the frequency domain where numerical errors can push one frequency higher then another.

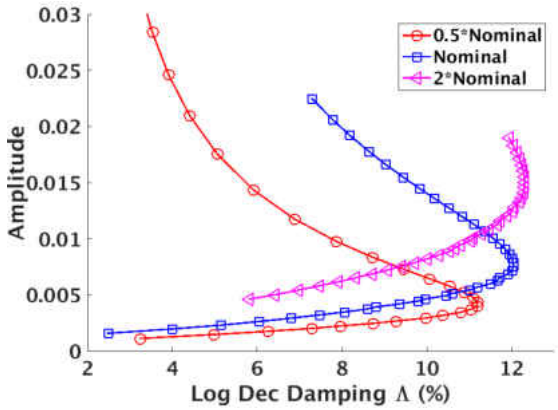

(a) Damp. vs Amp. w.r.t. Damper Mass

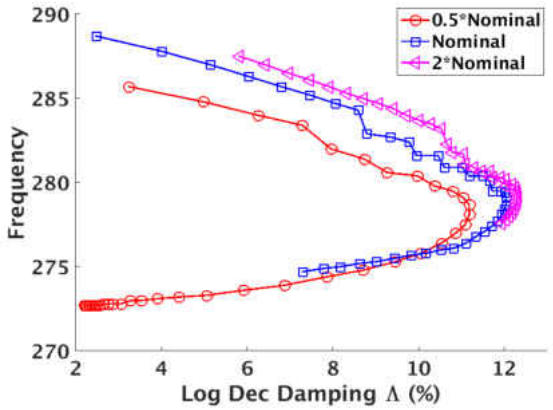

(b) Damp. vs Freq. w.r.t. Damper Mass

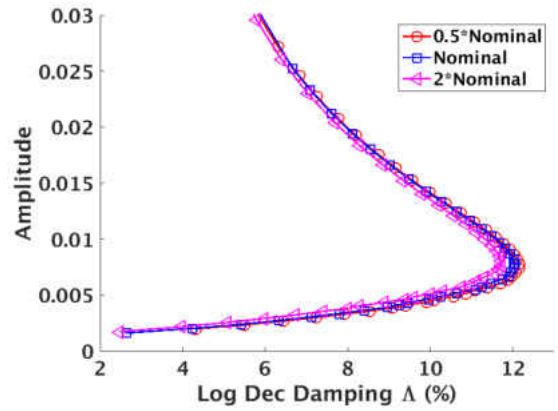

(c) Damp. vs Amp. w.r.t. Damper Roughness

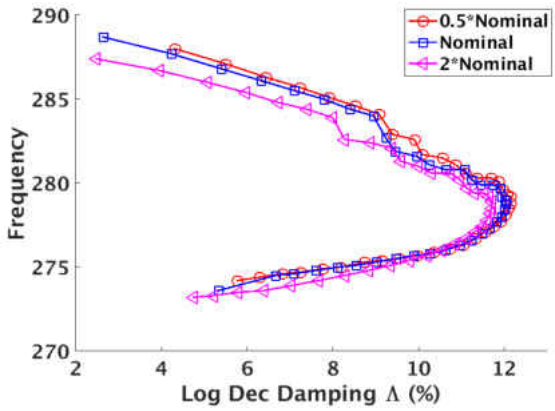

(d) Damp. vs Freq. w.r.t. Damper Roughness

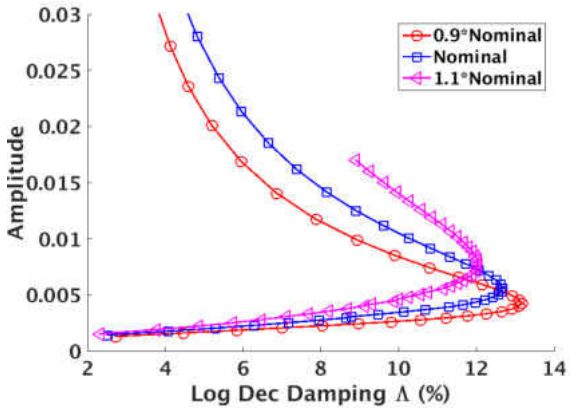

(e) Damp. vs Amp. w.r.t. Friction

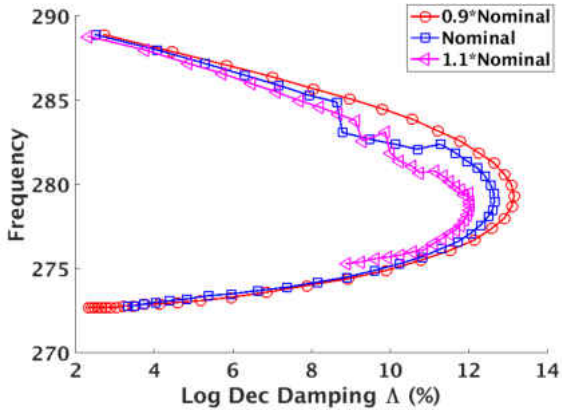

(f) Damp. vs Freq. w.r.t. Friction

Figure 4.9: Academic Geometry 2 Forced Response vs Design Parameter Variation

As with the first academic blade model, the impact the design parameters have on the excitation needed to generate the predicted forced response is shown next. The following plots in figure 4.10 show how the excitation changes for the predicted damping and amplitude with respect to variations in the design parameters. The plots show how the variation in the design parameters impact the excitation needed to generate the forced vibration response. Figures 4.10a-b show that as the damper mass increases, the excitation needed to generate the same predicted forced response increases. Figures 4.10c-d show that as the damper roughness has very little effect on the stimulus location of the maximum damping point. Figures 4.10e-f show that the stimulus of the maximum damping point increases with an increase in the friction coefficient in addition to the amplitude increasing.

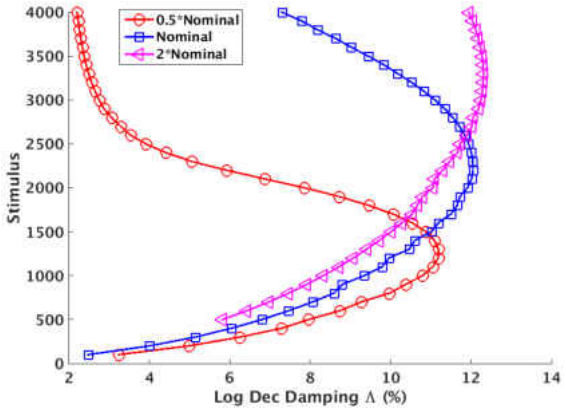

(a) Damping vs Stimulus w.r.t. Damper Mass

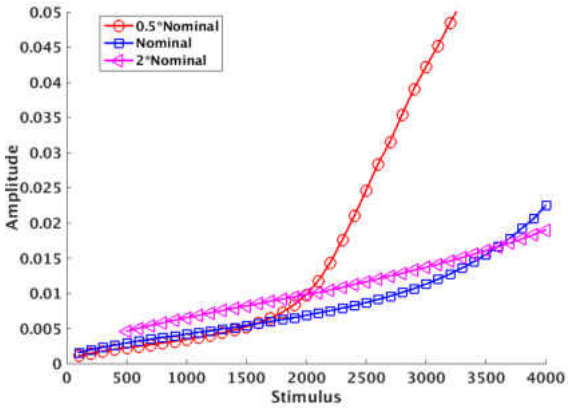

(b) Stimulus vs Amplitude w.r.t. Damper Mass

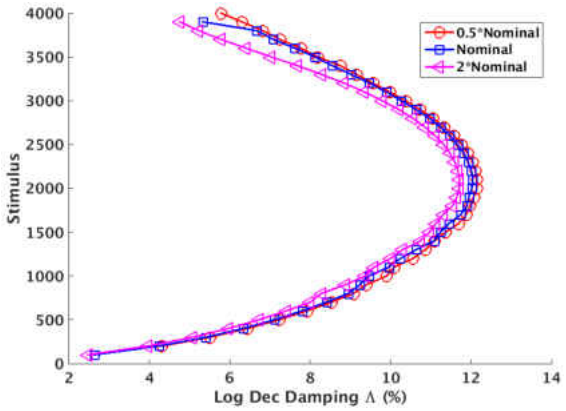

(c) Damp. vs Stim. w.r.t. Damper Roughness

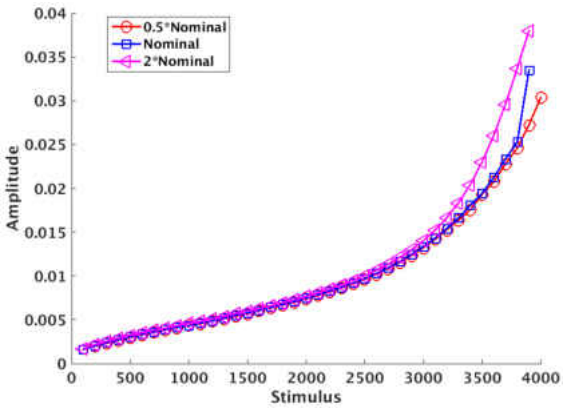

(d) Stim. vs Amp. w.r.t. Damper Roughness

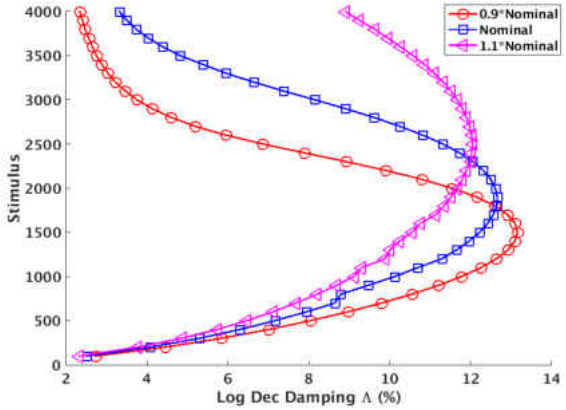

(e) Damping vs Stimulus w.r.t. Friction

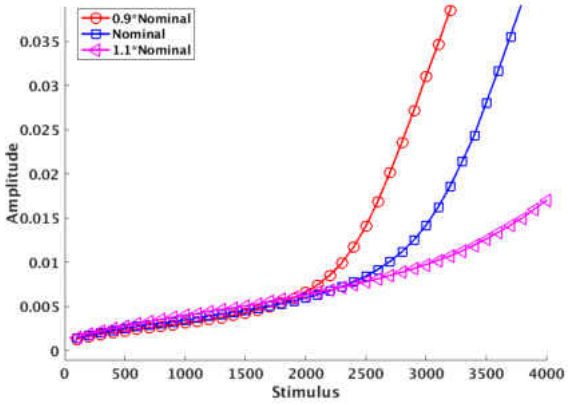

(f) Stimulus vs Amplitude w.r.t. Friction

Figure 4.10: Academic Geometry 2 Excitation vs Design Parmater Variations

The sensitivity of the second academic geometry to the design parameters across a range of reduced order models is compared next. The plots shown in figure 4.11 demonstrate how the predicted maximum damping, amplitude at maximum damping and frequency at maximum damping are affected by variations in the design parameters. The results in figure 4.11 are normalized with respect to the predicted damping, amplitude and frequency at the nominal design parameter value with respect to the 160 mode model, represented as one.

Figures 4.11a-c show the as the damper mass increases, the maximum damping and amplitude at maximum damping increase, while the frequency at maximum damping remains unchanged. Figures 4.11d-f indicate that as the damper surface roughness increases, the maximum damping decreases, the amplitude at maximum damping increases and the frequency at maximum damping remains relatively constant. Figures 4.11g-i demonstrate that as the friction coefficient increases, the maximum damping decreases, the amplitude at maximum damping increases and the frequency remains relatively unchanged.

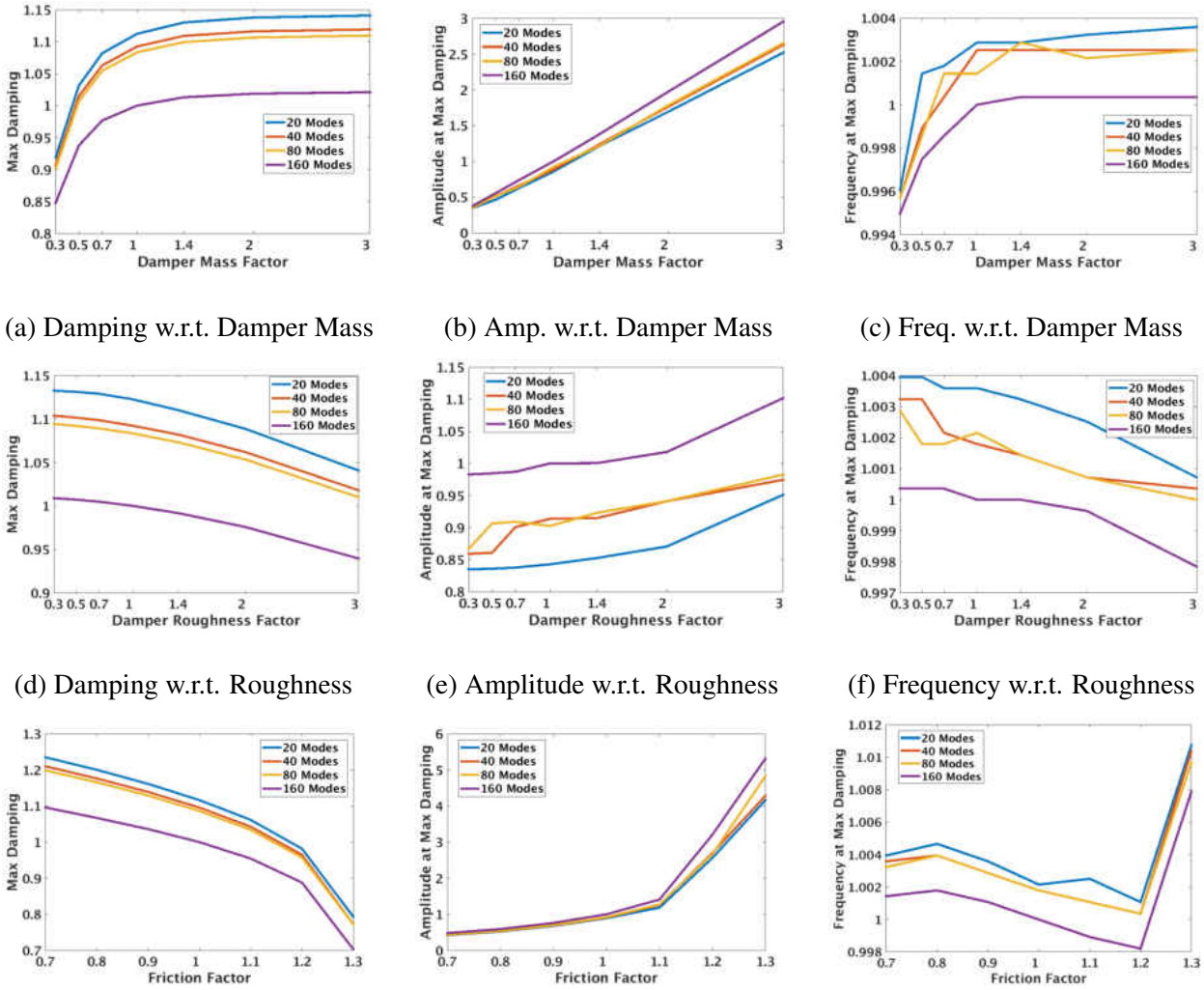

(a) Damping w.r.t. Damper Mass (b) Amp. w.r.t. Damper Mass (c) Freq. w.r.t. Damper Mass

(d) Damping w.r.t. Roughness (e) Amplitude w.r.t. Roughness (f) Frequency w.r.t. Roughness

(g) Damping w.r.t. Friction (h) Amplitude w.r.t. Friction (i) Frequency w.r.t. Friction

Figure 4.11: Sensitivity of Academic Geometry 2 to Design Parameter Variation

4.5 Comparisons of Academic Geometries 1 and 2

This section discusses the geometrical differences between the two academic geometries and compares the sensitivities of the blades responses to changes in the design parameters. The main

difference between the two blade models are the size of the blade sections and the broach angle. The first blade model has a blade section length of approximately 660 mm, while the second blade model has a blade section length of roughly 350 mm. Additionally the first blade model has no broach angle while the second blade geometry has a broach angle of 15°. Figure 4.12 compares the sensitivities of the two blade models to variations in the design parameters. The response of the blade models are normalized with respect to the value of the maximum damping, and amplitude at maximum damping at the nominal value of the design parameters. Based on the results in figure 4.12, variation in the damper mass has the largest impact on the predicted maximum damping and amplitude at maximum damping for both of the academic blades. The second academic blade is sensitive to changes in the friction coefficient, while the first geometry is insensitive. The first geometry is more sensitive to changes in the damper surface roughness then the second geometry.

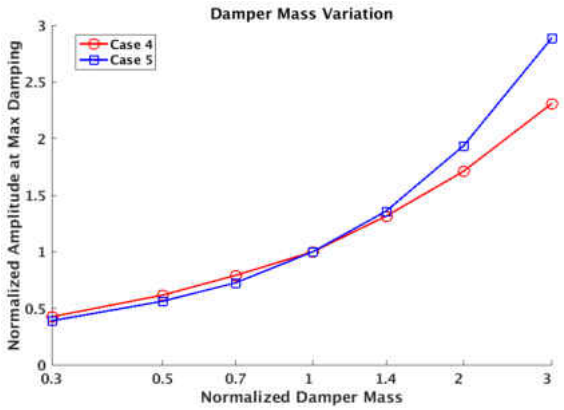

(a) Amplitude w.r.t. Damper Mass

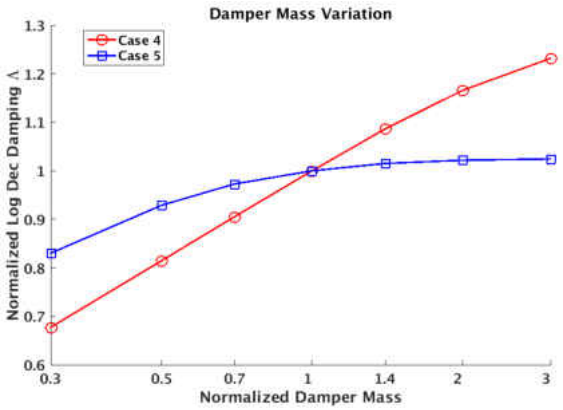

(b) Damping w.r.t. Damper Mass

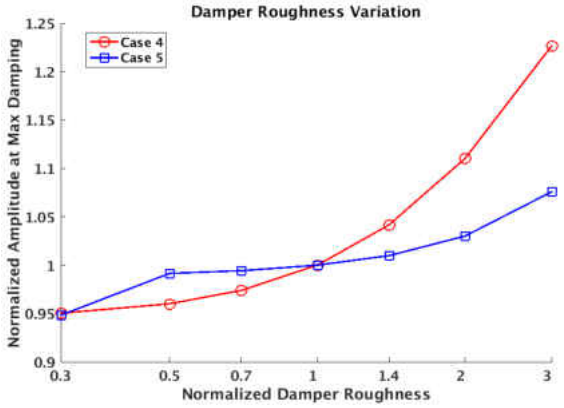

(c) Amplitude w.r.t. Friction

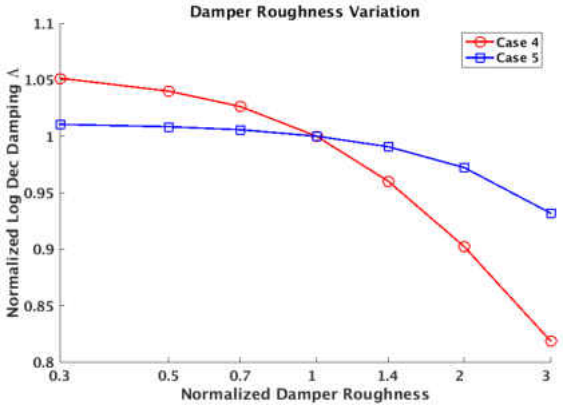

(d) Damping w.r.t. Damper Mass

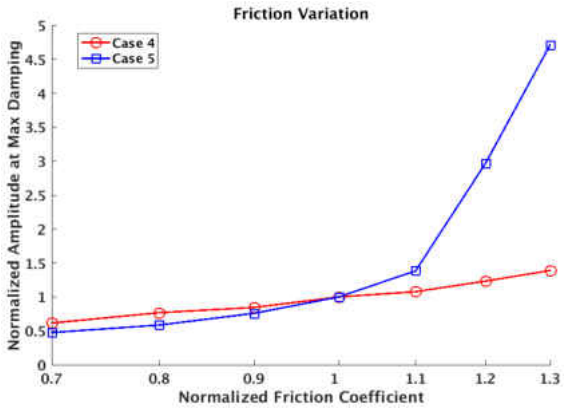

(e) Damping w.r.t. Damper Roughness

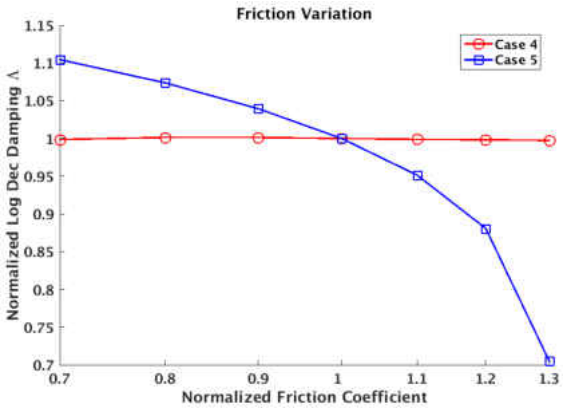

(f) Damping w.r.t. Friction

Figure 4.12: Comparison of Sensitivity of Academic Geometries to Design Parameters

Overall, the two blades display a qualitatively similar behavior when the damper mass, damper surface roughness, and the friction coefficient are varied. Figures 4.12a-b show that as the damper mass increases, the predicted maximum damping and amplitude at maximum damping increase. Figures 4.12c-d demonstrate that as the damper surface roughness increases, the maximum damping decreases, while the amplitude at maximum damping increases. Figures 4.12e-f show that as the friction coefficient increase, the maximum damping decreases, while the amplitude at maximum damping increases.

4.5.1 Nodal Displacements of Blade Models

During the development of the second academic blade geometry, the blade and damper system was not reaching a suitable damping level in the forced response; figure 4.13 shows the initial damping and amplitude response. To investigate the possible cause of this the nodal displacements of the blade leading edge and underplatform region were compared; table 4.1 shows the nodal displacements of the damper contact regions and blade leading edge tips. The ratio of the blade tip divided by the damper contact areas (found in table 4.1) was used to determine how coupled the motion is between the blade and platform. The lower this ratio is the more coupled the blade is to the platform. Typical blades in industry have a coupling ratio ranging from 20 to 40. It was found that the platform region of the second academic geometry was very stiff compared to the blade region; i.e. there was very little coupling between the blade tip motion and platform during vibration, leading to a low predicted damping response shown in figure 4.13.

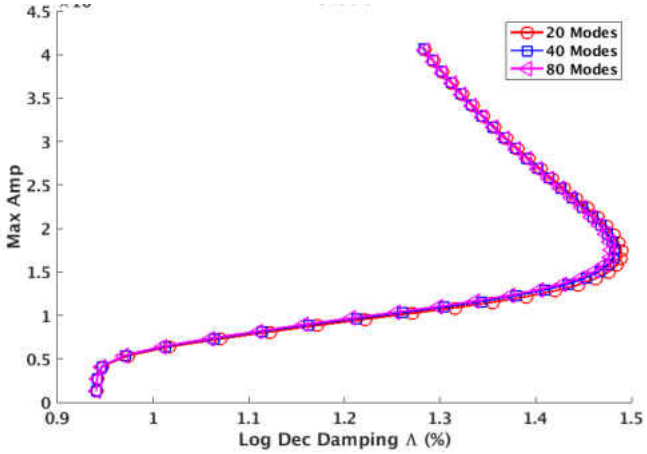

Figure 4.13: Initial Forced Response of Blade 2

Table 4.1: Academic Geometries Nodal Displacements

	Blade 1 Displacement (mm)	Blade 2 Displacement (mm)
Left Underplatform	0.169	0.069
Right Underplatform	0.197	0.054
Blade Leading Edge Tip	12.4	16.9
Blade Tip/Damper Contact	67.69	275

To solve this problem, the platform region of the blade needed to be less stiff, such that more motion from the blade profile would be transferred to the platform. The solution implented was to increase the the radial dimension of the platform region (R_1, R_2, and R_3) along the blade to make the blade root region less stiff. In other words the entire platform region was moved up along the blade. This leads to more relative motion between the blade and damper, which creates more friction and therefore more damping. Therefore there was more coupling between the blade and platform

regions of the second academic geometry; table 4.2 shows the updated nodal displacements using the new dimensions.

Table 4.2: Academic Geometry 2 Updated Nodal Displacements

	Blade 2 Displacement (mm)
Left Underplatform	0.333
Right Underplatform	0.263
Blade Leading Edge Tip	11.5
Blade Tip/Damper Contact	38.7

CHAPTER 5
CONCLUSIONS

Two academic turbine blade models coupled with underplatform dampers have been presented which are representative of industrial turbine blades. The academic models display qualitatively similar behavior to industrial counterparts when the number of modes in a modal analysis is varied. The academic models also have been demonstrated to show similar behavior under sensitivities to design parameters.

The comparison of the academic blade models revealed that the first academic blade is more sensitive to variations in the design parameters. The behavior of the blade models to variations in the design parameters are summarized as follows. When the damper mass increases, the predicted maximum damping increases, and the amplitude at maximum damping increases. Increasing the damper surface roughness decreases the predicted maximum damping, and increases the amplitude at maximum damping. As the friction coefficient increases, the predicted maximum damping decreases while the amplitude at maximum damping increases.

Additionally, the variations in the design parameters also influenced the required excitation needed to reach the maximum damping point of the system and are summarized as follows. Increasing the damper mass and friction coefficient increases the excitation point of the maximum damping. On the other hand, varying the surface roughness of the contact between the damper and

blade platform has almost no influence on the excitation needed to reach the maximum damping point of the system.

The main goal of the presented academic blade models is for them to be used for further academic analysis to act as a standard for comparison of forced response within the turbomachinery community. The presented blade models and accompanying underplatform dampers have demonstrated qualitatively similar behavior to complex industrial blade models. As new model reduction, nonlinear damping and forced response algorithms and forced response algorithms, these blade models provide an academic test case which can help bridge the gap to industry with highly complex blades.

5.1 Lessons Learned

During the course of the development of the blade and damper geometries there were a numerous speed bumps along the way, where problems came up and investigations into the solutions developed an increased insight into the design of the academic turbine blade models. This section discusses those speed bumps and the insights that were gained upon reaching solutions to those problems.

During the initial characterization of the blade models it was difficult to get forced response results in the nonlinear code DATAR. It was later found to be due to low forcing since point loads were used to excite the academic blade models; these point loads needed to be drastically scaled up (100% - 1000%) within DATAR in order to get a response whereas the full pressure loads used on

the industry models require very little scaling for a response (1% - 3%). Essentially the point load simplification of the excitation needs to be drastically scaled in magnitude when compared with the full pressure loads used in the industry blade models. However, the forced vibration response results are not dependent on the excitation itself, just the magnitude.

The mesh density of the platform regions of the blade models where the contact interface between the blade and damper occurs was found to be important in the forced vibration response prediction. As was mentioned in the results section for the first academic blade model, the initial characterization of the blade displayed oscillatory convergence behavior between the reduced order models with respect to the sensitivities to the design parameters which was unexpected behavior based. However, once the mesh of the platform region was increased, the reduced order models of the blade model with respect to sensitivities to design parameters displayed monotonic convergence which was expected. This result reinforces the idea that any contact interfaces within the model need to maintain a certain fidelity in order to accurately capture the behavior, even with the simple academic blade models presented in this thesis.

Due to the simplicity in design of the academic blade models there is poor coupling between the motion of the blade profile above the platform and the platform regions of the blade. While this was expected and known before hand, it was not until investigating and comparing the nodal displacements of the blade tip and underplatform nodes in the finite element model that the extent of the poor coupling was discovered. This investigation provided insight into designing the platform and blade root regions of the academic blade models to allow for more vibration to be transferred from the vibration of the blade tip to platform region. This occurred during the design of the sec-

ond academic geometry, the blade root region was too stiff leading to essentially no damping in the forced response results because the platform was not vibrating and the damper unable to dissipate energy. The update to the geometry involved increasing the length of the blade root section in the radial direction as well as increasing where the platform region was on the blade model. This change in geometry lead to an increased coupling between the blade tip and platform regions to allow for sufficient predicted damping in the forced vibration results.

5.2 Future Work

The academic geometries presented here are good candidates as a first point of comparison for methods in model reduction and forced vibration response of turbine blades coupled with underplatform dampers. The academic geometries have been shown to behave qualitatively similar to respective industrial counterparts and could act as test cases for new developments in the forced vibration response community, to compare with the results presented in this paper. However, the blade and damper geometries themselves are not physically realistic to those seen industry. The blade profiles of the academic geometries are essentially solid cantilever beams, which is why the underplatform dampers are relatively large. A second generation blade could incorporate more complexity into the blade profile portion to be more in line with blade designs seen in industry and therefore lead to more realistic underplatform damper models. One large disparity between these presented blade models and industry blades are the complex blade profiles used in industry. A more complex blade design in a second generation academic model (i.e. not solid blades as one

option) could alleviate the need for a relatively large underplatform damper. The academic blade models have the majority of their mass in the blade sections, whereas the industrial counterparts have their mass more equally distributed between the blade profile and platform regions.

Recently researchers have been using a Lagrangian method to enforce contact at friction interfaces, whereas previous methods and the one used here used contact stiffness terms to enforce contact. Methods using contact stiffness terms are highly sensitive to values input for them and these stiffness terms themselves are poorly understood, however they due produce similar results to the Lagrangian methods. The proposed academic blades presented here are great candidates for conducting forced vibration response method utilizing Lagrangian methods for enforcing contact and comparing with the results presented here. Comparing the results presented here with an alternative Lagrangian method is of interest to the author.

Ultimately the long term goal of the presented academic turbine blade models is for the use as a point of comparison in the predicted forced vibration response community. These blade models have been shown to behave qualitatively similar to that of industrial turbine blades, however the academic blade models are not intended to be used to aid in the design of blade/damper systems. The presented models have a relatively simple design in terms of academia while still requiring a relatively large amount of modes for convergence. This simple geometry allows for a more fundamental investigation into the model reduction process and forced response technique to investigate the convergence behavior that is still a critical factor in the analysis of high-fidelity blades with reduced order models.

APPENDIX A
ACADEMIC BLADE 1 ANSYS MECHANICAL APDL CODE

```
!! Academic blade 1 ANSYS Macro UCF

/PREP7


!! Material Properties of Blade

ED_B = 200000      !!    E-DYN. Platform

NU_B =      0.250

MU   =      0.33   !!    Friction Coeff.

dens = 8E-09

mp,  ex,1,ED_B    !!  Define Material Models and Properties

mp,nuxy,1,NU_B

mp,dens,1,DENS

mp,  ex,2,ED_B    !!  Define Material Models and Properties

mp,nuxy,2,NU_B

ET,1,SOLID187,,,,,,,


!! Blade dimensions

N = 45

R0 = 850

R1 = 905

R4 = 1600
```

```
!! h defined as blade thickness (constant if no taper used)
h = 50

!! Blade root thickness
Troot = 50

!! Variable x here used to define half the length of the blade taper since
!! blade symmetric about y-axis
x=h/12

pi=asin(1)*2
Adisk = 2*pi/N

! Calculated from non-linear equations defining model

psi_r = 0.0527
psi_l = 0.0860
R2 = 928
R3 = 938

!! Equations which define key points of blade from cylindrical to cartesian
```

```
R0y = R0*R0-Troot*Troot*0.25

R1y = R1*R1-Troot*Troot*0.25


R2yl = R2*cos(psi_l)

R2xl = R2*sin(psi_l)


R2yr = R2*cos(psi_r)

R2xr = R2*sin(psi_r)


R3yl = R3*cos(psi_l)

R3xl = R3*sin(psi_l)


R3yr = R3*cos(psi_r)

R3xr = R3*sin(psi_r)


R3b = R3*R3-h*h*0.25


R4b = R4*R4-x*x


!! Local coordinate systems defined to orientate the blade
```

```
LOCAL,11,1, 0, 0, 0, 1.8E+02, 0, 2.7E+02


!! Begining construction of blade


csys,0

k,,,-Troot/2,sqrt(R0y)

k,,,Troot/2,sqrt(R0y)

k,,,-Troot/2,sqrt(R1y)

k,,,Troot/2,sqrt(R1y)


k,,,R2xr,R2yr

k,,,-R2xl,R2yl


k,,,-R3xl,R3yl

k,,,R3xr,R3yr


k,,,h/2,sqrt(R3b)

k,,,-h/2,sqrt(R3b)


k,,,x,sqrt(R4b)
```

```
k,,,-x,sqrt(R4b)


csys,11

l,1,2


csys,0

l,7,10

l,9,8

l,1,3

l,3,6

l,7,6

l,2,4

l,4,5

l,5,8


csys,0


l,10,12

l,12,11

l,11,9
```

```
!! Creating an area on underplatform to goup nodes later

KL,8,1-0.4, ,

KL,8,1-0.6, ,

ldel,8

l,4,14

l,14,13

l,13,5


!! Creating an area on underplatform to grab nodes for grouping

KL,5,1-0.69, ,

KL,5,1-0.4, ,

ldel,5

l,3,15

l,15,16

l,16,6


!! Selecting lines making up blade and platform

lsel,s,line,,all

al,all


!! Extruding blade and platform, then setting the mesh attributes
```

```
VOFFST,1,-300, ,

VATT,1,,1, 0

MSHAPE,1,3D

MSHKEY,0


!! Creating Massless disk for cyclic symmetry generation

k,,,200*sin(Adisk/2),200*cos(Adisk/2)

k,,,-200*sin(Adisk/2),200*cos(Adisk/2)


k,,,R0*sin(Adisk/2),R0*cos(Adisk/2)

k,,,-R0*sin(Adisk/2),R0*cos(Adisk/2)


csys,11

l,34,33

l,36,35


csys,0

l,34,36

l,33,35


!! Sellecting lines making up disk for extrusion
```

```
lsel,s,line,,49,52

al,all

VOFFST,19,-300, ,


!! Selecting disk volume to set mesh attributes and mesh the volume

vsel,,,,2

VATT,2,,1,0

VMESH,2

allsel


!! Meshing the blade and platform

VMESH,1


!! Selecting the platform areas for mesh refinement

asel,s,area,,1,2

asel,a,area,,4,9

asel,a,area,,13,18

AREFINE,all,,3


allsel
```

```
dsys,0

csys,0


!! Applying boundary conditions to blade, fixing the root and applying point load

!! to LE tip transverse to blade for modal excitation

DA,3,ALL

DA,21,all

F,21415,FY,100
```

APPENDIX B
ACADEMIC BLADE 2 ANSYS MECHANICAL APDL CODE

```
!Academic Blade 2 ANSYS APDL Macro UCF

/PREP7


! Number of blades

N = 60


!!  Define Material Models and Properties

ED_B = 200000      !!    E-DYN. Platform

NU_B =      0.250

MU   =      0.33   !!    Friction Coeff.

dens = 8E-09


mp,  ex,1,ED_B

mp,nuxy,1,NU_B

mp,dens,1,DENS

mp,  ex,2,ED_B    !!  Define Material Models and Properties

mp,nuxy,2,NU_B

ET,1,SOLID187,,,,,,,


!! Define Geometrical variables of blade and platform

R0 = 800
```

```
R1 = 825

R4 = 1200


*afun,rad

pi=asin(1)*2


broach=15*pi/180


h=50

Troot = 50


!! x-value determines the taper 2*x = value of span of blade tip

!! no taper used here

x=h/2


!! Calculated Inputs

! Value in radians of disk sector

Adisk = 2*pi/N


! Calculated from Matlab non-linear equations
```

```
psi_r = 0.0519

psi_l = 0.0519

R2 = 842

R3 = 852


!! Defining broach angle csys 11 (-15 degrees about global y in this case)


csys,0

k,,0,0

k,,cos(broach),-sin(broach),0

k,,0,1,0

CSKP,13,0,1,2,3


LOCAL,11,1,0,0, 0,1.8E+02,0,2.7E+02

LOCAL,12,0, 0, 0, 0, 1.80E+02, 0, 2.7E+02



! Creating parameters which are used to define blade profile keypoints


R0y = R0*R0-Troot*Troot*0.25

R1y = R1*R1-Troot*Troot*0.25
```

```
R2yl = R2*cos(psi_l)

R2xl = R2*sin(psi_l)


R2yr = R2*cos(psi_r)

R2xr = R2*sin(psi_r)


R3yl = R3*cos(psi_l)

R3xl = R3*sin(psi_l)


R3yr = R3*cos(psi_r)

R3xr = R3*sin(psi_r)


R3b = R3*R3-h*h*0.25


R4b = R4*R4-x*x


!! Begin defining keypoints of platform

csys,0


k,,,-Troot/2,sqrt(R0y)
```

```
k,,,Troot/2,sqrt(R0y)

k,,,-Troot/2,sqrt(R1y)

k,,,Troot/2,sqrt(R1y)

k,,,R2xr,R2yr

k,,,-R2xl,R2yl

k,,,-R3xl,R3yl

k,,,R3xr,R3yr


!! Connect keypoints with lines/arcs

csys,11

l,4,5


csys,12

l,4,6

l,6,9

l,10,9

l,5,7

l,7,8

l,8,11

l,10,11
```

```
!! Creating lines to define damper contact node


KL,3,1-0.6, ,

KL,3,1-0.4, ,

ldel,3

l,6,12

l,12,13

l,13,9


KL,6,1-0.6, ,

KL,6,1-0.4, ,

ldel,6

l,7,14

l,14,15

l,15,8


!! Extrude platform area in local cylindrical using VEXT, allows platform

!! to conform to disk profile best

csys,11

lsel,s,line,,all

al,all
```

```
VEXT,1,,,0,-3.8,-193.2,1,1,1

VATT,       1, ,   1,       0


!! Define blade profile keypoints in broach frame

csys,13


!! Blade base points defined a little below to be inside platform

!! to add the blade volume to platform later since they were built separately

k,,-7,h/2,sqrt(R3b)-10

k,,-7,-h/2,sqrt(R3b)-10


k,,-7,x,sqrt(R4b)

k,,-7,-x,sqrt(R4b)


!! Connect blade keypoints with lines


l,28,29

l,29,31

l,31,30

l,30,28
```

```
lsel,s,line,,37,40

al,all

VATT,       1, ,   1,       0

VOFFST,15,186.2,,


!! Add volumes of extruded platform and blade

VADD,1,2

VATT,       1, ,   1,       0

VMESH,3


!! Creating massless disk for expansion


csys,0


k,,,200*sin(Adisk/2),200*cos(Adisk/2)

k,,,-200*sin(Adisk/2),200*cos(Adisk/2)


k,,,R0*sin(Adisk/2),R0*cos(Adisk/2)

k,,,-R0*sin(Adisk/2),R0*cos(Adisk/2)


csys,11
```

```
l,29,28

l,33,32



csys,0

l,29,33

l,28,32



csys,11

lsel,s,line,,37,38

lsel,a,line,,40,41

al,all


! Extruding massless disk section


VEXT,9,,,0,-3.8,-193.2,1,1,1

vsel,s,volu,,1

VATT,       2, ,   1,       0

VMESH,1
```

```
allsel


dsys,0

csys,0


!! Applying fixed blade root boundary condition and point force

!! transverse to LE blade tip for modal excitation


DA,3,ALL

DA,16,ALL

F,2394,FY,100
```

LIST OF REFERENCES

[1] Petrov EP (2011) "A high-accuracy model reduction for analysis of nonlinear vibrations in structures with contact interfaces," *Journal of Engineering for Gas Turbines and Power* 133 (10): 102503. doi:10.1115/1.4002810

[2] Zucca S, Firrone CM, Gola M (2013) "Modeling underplatform dampers for turbine blades: a refined approach in the frequency domain," *Journal of Vibration and Control* 19 (7): 1087–1102. doi:10.1177/1077546312440809

[3] Yang BD, Menq CH (1998) "Characterization of contact kinematics and application to the design of wedge dampers in turbomachinery blading: Part 2 – prediction of forced response and experimental verification," *Journal of Engineering for Gas Turbines and Power* 120 (2): 418–423. doi:10.1115/1.2818139

[4] Firrone CM, Zucca S (2011) "Modelling friction contacts in structural dynamics and its application to turbine bladed disks," pages 301–334 in in *Numerical Analysis – Theory and Applications*; Awrejcewicz J (editor),. doi:10.5772/25128

[5] Nacivet S, Pierre C, Thouverez F, Jezequel L (2003) "A dynamic lagrangian frequency-time method for the vibration of dry-friction-damped systems," *Journal of Sound and Vibration* 265 (1): 201–219. doi:10.1016/S0022-460X(02)01447-5

[6] Laxalde D, Thouverez F (2009) "Complex non-linear modal analysis for mechanical systems: Application to turbomachinery bladings with friction interfaces," *Journal of Sound and Vibration* 322 (4–5): 1009–1025. doi:10.1016/j.jsv.2008.11.044

[7] Anna Herzog, Malte Krack LP, Wallaschek J (2014) "Comparison of two widley-used frequency-time dontmain contact models for the vibration simulation of shrouded turbine blades," *Proceedings of ASME 2014 Turbo Expo: Turbine Technical Conference and Exposition*, GT2014-26226.

[8] Petrov EP, Ewins DJ (2003) "Analytical formulation of friction interface elements for analysis of nonlinear multi-harmonic vibrations of bladed disks," *Journal of Turbomachinery* 125 (2): 364–371. doi:10.1115/1.1539868

[9] Griffin JH (1990) "A review of friction damping of turbine blade vibration," *International Journal of Turbo and Jet Engines* 7 (3–4): 297–308. doi:10.1515/TJJ.1990.7.3-4.297

[10] Slater J, Minkiewicz G, Blair A (1998) "Forced response of bladed disk assemblies – a survey," *Proceedings of the Thirty-Fourth AIAA/ASME/SAE/ASEE Joint Propulsion Conference*, AIAA 98-3743. doi:10.2514/6.1998-3743

[11] Menq CH, Griffin JH, Bielak J (1986) "The influence of a variable normal load on the forced vibration of a frictionally damped structure," *Journal of Engineering for Gas Turbines and Power* 108 (2): 300–305.

[12] Menq CH, Bielak J, Griffin JH (1986) "The influence of microslip on vibratory response, part ii: A comparison with experimental results," *Journal of Sound and Vibration* 107 (2): 295–307. doi:10.1016/0022-460X(86)90239-7

[13] Greenwood JA, Williamson JBP (1966) "Contact of nominally flat surfaces," *Proceedings of the Royal Society of London A: Mathematical, Physical and Engineering Sciences* 295 (1442): 300–319. doi:10.1098/rspa.1966.0242

[14] Yang BD, Menq CH (1998) "Characterization of contact kinematics and application to the design of wedge dampers in turbomachinery blading: Part 1 – stick-slip contact kinematics," *Journal of Engineering for Gas Turbines and Power* 120 (2): 410–417. doi:10.1115/1.2818138

[15] Tworzydlo W, Cecot W, Oden J, Yew C (1998) "Computational micro- and macroscopic models of contact and friction: formulation, approach and applications," *Wear* 220 (2): 113 – 140. doi:http://dx.doi.org/10.1016/S0043-1648(98)00194-X

[16] Sextro W (2000) "The calculation of the forced response of shrouded blades with friction contacts and its experimental verification," *Proceedings of ASME 2000 Turbo Expo: Power for Land, Sea, and Air*, 2000-GT-0540. doi:10.1115/2000-GT-0540

[17] Allara M (2009) "A model for the characterization of friction contacts in turbine blades," *Journal of Sound and Vibration* 320 (3): 527–544. doi:10.1016/j.jsv.2008.08.016

[18] Cardona A, Coune T, Lerusse A, Geradin M (1994) "A multiharmonic method for non-linear vibration analysis," *International Journal for Numerical Methods in Engineering* 37 (9): 1593–1608. URL: http://dx.doi.org/10.1002/nme.1620370911 doi:10.1002/nme.1620370911

[19] Pesheck E, Boivin N, Pierre C, Shaw SW (2001) "Nonlinear modal analysis of structural systems using multi-mode invariant manifolds," *Nonlinear Dynamics* 25 (1–3): 183–205. doi:10.1023/A:1012910918498

[20] Panning L, Sextro W, Popp K (2000) "Optimization of interblade friction damper design," *Proceedings of ASME 2000 Turbo Expo: Power for Land, Sea, and Air*, 2000-GT-0541. doi:10.1115/2000-GT-0541

[21] Panning L, Sextro W, Popp K (2002) "Optimization of the contact geometry between turbine blades and underplatform dampers with respect to friction damping," *Proceedings of ASME 2000 Turbo Expo: Power for Land, Sea, and Air*, GT-2002-30429. doi:10.1115/GT2002-30429

[22] Panning L, Popp K, Sextro W, Gotting F, Kayser A, Wolter I (2004) "Asymmetical underplatform dampers in gas turbine bladings: Theory and application," *Proceedings of ASME 2004 Turbo Expo: Power for Land, Sea, and Air*, GT2011-53316. doi:10.1115/GT2004-53316

[23] Siewert C, Panning L, Schmidt-Fellner A, Kayser A (2006) "The estimation of the contact stiffness for diretly and indirectly coupled turbine blades," *Proceedings of ASME 2006 Turbo Expo: Power for Land, Sea and Air*, GT2006-90473. doi:10.1115/GT2006-90473

[24] Krack M, Panning L, Wallaschek J, Siewert C, Hartung A (2012) "Robust design of friction interfaces of bladed disks with respect to parameter uncertainties," *Proceedings of ASME Turbo Expo 2012*, GT2012-68578. doi:10.1115/GT2012-68578

[25] Krack M, Panning-von Scheidt L, Wallaschek J (2013) "A high-order harmonic balance method for systems with distinct states," *Journal of Sound and Vibration* 332 (21): 5476–5488. doi:10.1015/j.jsv.2013.04.048

[26] Deshmukh DV, Berger EJ, Mackin TJ, Inglis H (2005) "Convergence behaviors of reduced-order models for frictional contacts," *Journal of Vibration and Acoustics* 127 (4): 370–381. doi:10.1115/1.1924645

[27] Petrov EP (2004) "Method for direct parametric analysis of nonlinear forced response of bladed disks with friction contact interfaces," *Journal of Turbomachinery* 126 (4): 654–662. doi:10.1115/1.1776588

[28] Schwingshackl CW, Petrov EP, Ewins DJ (2012) "Effects of contact interface parameters on vibration of turbine bladed disks with underplatform dampers," *Journal of Engineering for Gas Turbines and Power* 134 (3): 032507. doi:10.1115/1.4004721

[29] Schwingshackl CW, Petrov EP, Ewins DJ (2012) "Measured and estimated friction interface parameters in a nonlinear dynamic analysis," *Mechanical Systems and Signal Processing* 28 (8): 574–584. doi:10.1016/j.ymssp.2011.10.005